

5. FORMULATION DEVELOPMENT AND CHARACTERIZATION OF PLHNCs

PART A: FORMULATION OF FULVESTRANT LOADED PLHNCs

5.1 Introduction

Polymer lipid hybrid nanocarriers are mainly prepared by four different techniques as described in Chapter 2, but mainly two techniques are widely used due to their effectiveness and higher yield (1). One technique includes a two-step procedure in which the polymer core and lipid shell are separately prepared and then inserted and blended, and the other technique involves a single-step process in which the hybrid nanoparticles are prepared using a single-step system of nanoprecipitation and self-assembly (2). The suitability of various methods described in Chapter 2 was tested and the best approach appropriate for the preparation of Fulvestrant PLHNCs with favourable features was further optimized. The particle size and encapsulation efficiency were selected as quality target. Plackett-Burman design (PBD) and Box-Behnken design (BBD) were employed as the statistical design to fully elucidate the formulation development parameters. Further, the optimized PLHNCs formulation was subjected to lyophilization using various cryoprotectants to increase drug retention (3).

5.2 Screening of Method of preparation

Table 5.1 Preliminary screening of method of preparation

Sr. No.	Method	Particle Size (nm)	Encapsulation Efficiency (%)	PDI
1.	Single step emulsification method	341.2 ± 12.65	52.81 ± 2.63	0.523 ± 0.094
2.	Two step method	215.6 ± 3.51	65.24 ± 3.58	0.336 ± 0.056
3.	Emulsification solvent evaporation	446.1 ± 15.08	47.32 ± 5.24	0.638 ± 0.116
4.	Single step nanoprecipitation	168.3 ± 2.26	73.65 ± 2.88	0.318 ± 0.052

5.3 Formulation and Development

5.3.1 Method of preparation

Based on preliminary screening, formulations of PLHNCs were performed using modified single-step nano-precipitation method which involves self-assembly of polymers and various ratios of lipids. Two phases (organic and aqueous) were prepared separately and then, mixed to form PLHNCs (4). A fixed quantity of PLGA 75:25 (1 – 10 mg/ml) and Fulvestrant were dissolved in acetonitrile to prepare the organic phase. SPC – 3: DOPE: DSPE-PEG₂₀₀₀ were dissolved in 4% ethanolic solution to form aqueous phase. The resultant solution was heated at 65°C to ensure the phase transition of the lipid-bi-layer, when mixed further(5). After that, Fulvestrant containing PLGA solution was added to the preheated lipid solution via dropwise method at 1mL/min flow rate under vigorous mixing at 200 to 2000 rpm until complete evaporation of the organic solvent and maximum encapsulation of Fulvestrant in PLHNCs. Furthermore, PLHNCs suspension was passed through laboratory manual extruder in order to improve the particle size distribution and polydispersity index (4).

Selection of a phospholipid has been a major control parameter to maintain the stability as well as the encapsulation of drug in polymer core and strengthen the outer core to prevent the leakage of the drug from its core-coat system. To target the formulation towards the tumor cells it is required to be attached with a suitable ligand and folic acid is found to be overexpressed in most of the breast cancer types. For preparation of folate conjugated PLHNCs, DSPE-PEG-FA was used instead of DSPE-PEG following the same nanoprecipitation method explained above (6).

5.3.2 Preliminary screening study for formulation and process parameters

Polymer selection, amount of polymer, lipid composition, polymer to lipid ratio and drug input were identified as formulation factors, while stirring time, stirring speed and extrusion cycle were identified as process parameters that may alter quality profile of product (7). Fulvestrant loaded nanoparticulate formulation is expected to provide a better therapeutic index due to carrier facilitated intracellular transportation as well as the targeting effect. For these reasons, the target profile of the intended Fulvestrant PLHNCs was : (1) relatively high drug encapsulation efficiency (2) particle size below 200 nm and (3) sufficient stability on storage (8).

5.3.3 Selection of polymer

Polymeric nanoparticles were formed by single step nanoprecipitation in which different polymers (i.e., Polycaprolactone, Poly lactic acid, PEI, PLGA (50:50), PLGA (75:25) were dissolved in suitable solvent along with 10% w/w of Fulvestrant. Resulting organic phase was injected in aqueous phase containing 0.5 % Poloxamer 407 as a surfactant Organic solvent was allowed to evaporate, and nanoparticle drug suspension was obtained (9).

Table 5.2 Selection of polymer

Polymer (10 mg/ml)	Size (nm)	PDI	Entrapment Efficiency (%)
Polycaprolactone (PCL)	358.7 ± 9.34	0.418 ± 0.17	38.4 ± 2.63
Poly lactic acid (PLA)	413.6 ± 13.68	0.356 ± 0.21	43.2 ± 1.86
Poly glycolic acid (PGA)	363.4 ± 7.65	0.384 ± 0.19	45.1 ± 2.29
Poly D,L-lactic-co-glycolic acid (PLGA) (75:25)	116.5 ± 3.17	0.218 ± 0.08	68.5 ± 3.17
Poly D,L-lactic-co-glycolic acid (PLGA) (50:50)	163.4 ± 5.64	0.316 ± 0.14	55.2 ± 2.24
Polyethyleneimine (PEI)	276.6 ± 6.84	0.328 ± 0.26	41.4 ± 1.67
Chitosan	329.2 ± 3.85	0.527 ± 0.28	48.2 ± 2.13

From various polymers, PLGA (75:25) was selected for the preparation of PLHNCs based on encapsulation efficiency, size, and PDI. PLGA (75:25) showed the highest entrapment of Fulvestrant among all the polymers (Table 5.2). The highest entrapment of Fulvestrant in PLGA (75:25) might be due to higher hydrophobicity of polymer, based on the principle of like dissolves like which incorporates the drug rapidly into its core (10).

The particle size of the PLGA nanoparticles was found to be below 150 nm. Nanoparticles in the range of **100–200 nm** have been shown to extravasate through vascular fenestrations of tumors (the EPR effect) and escape filtration by liver and spleen (11). As size increases beyond 150 nm, more and more nanoparticles are entrapped within the liver and spleen, hence PLGA (75:25) was chosen for the further optimization.

5.3.4 Effect of polymer concentration on encapsulation efficiency and particle size:

As presented in Table 5.3, increasing the concentration of PLGA resulted in increased encapsulation efficiency of Fulvestrant. At high polymer concentration, the internal core volume for drug encapsulation was high which led to a higher encapsulation efficiency. At low polymer concentration, lower encapsulation of drug was reported, which suggested insufficient hydrophobic core to entrap the drug. With increasing concentration of polymer, gradual increase in encapsulation efficiency and reduction in particle size was noted up to 8 mg/ml. After 8 mg/mL polymer concentration, reduction in drug encapsulation and increase in particle size was observed. These effects explain another phenomenon that there could be an inverse relation between polymer concentration and drug encapsulation after saturation of the hydrophobic core. As the polymer concentration increased, zeta potential of the PLHNCs shifted from positive to negative charge due to negative charge of the PLGA.

Table 5.3 Effect of polymer concentration on encapsulation

Sr No.	Polymer concentration (mg/mL)	Encapsulation Efficiency (%)	Size (nm)	Zeta Potential (mV)
1	2	28.51 ± 1.24	314.6 ± 12.36	10.8 ± 1.6
2	4	33.28 ± 2.21	276.5 ± 11.67	4.9 ± 1.1
3	6	46.84 ± 3.18	215.3 ± 10.23	-3.4 ± 0.5
4	8	65.61 ± 3.68	121.2 ± 6.52	-10.9 ± 0.8
5	10	55.17 ± 2.86	188.7 ± 8.34	-14.5 ± 2.1
6	12	46.21 ± 2.32	241.8 ± 11.32	-17.6 ± 2.7

5.3.5 Effect of lipid to polymer ratio on drug encapsulation and particle size

The lipids for the formulation of PLHNCs were selected based on formulation parameters and route of administration. As the formulation is to be delivered by parenteral route and requires having pH specificity to acidic environment, the lipids compatible with injectables route and having pH sensitive properties were selected. Dioleoylphosphatidylethanolamine (DOPE) is the only lipid that has pH sensitive drug delivery ability in acidic pH, and the pH at tumor interface is 5.5. The inability of DOPE to give structural stability itself makes it difficult to form nanocarriers with DOPE alone, so soyabean phosphatidyl choline (SPC-3) was selected as supporting lipid for structural stability of DOPE based nanocarriers. The reason behind the

selection SPC is its stability in blood, compatibility with DOPE, biocompatibility, and wide application in intravenous delivery. DSPE-PEG₂₀₀₀ was selected as the secondary lipid to impart hydrophilicity to the nanoparticulate coat to prevent clearance of nanoparticles by RES and prolong the circulation of nanoparticles in vivo. The mole fraction of DOPE:SPC-3:DSPE-PEG₂₀₀₀ also plays important role in structural stability, circulation and syringeability. Though their mole fraction is selected based on CMC of lipids as their concentration beyond CMC will form micellar aggregates and nanoparticles separately. The CMC for DOPE is 300 μ M, for SPC-3 it is 500 μ M and for DSPE-PEG₂₀₀₀ its 200 μ M. So, for preparation of PLHNCs, for internal lipid, the amount of DOPE:SPC-3:DSPE-PEG₂₀₀₀ was kept 0.9 mg/ml, 1.5mg/ml and 0.6mg/ml respectively .

From Table 5.4, the percentage weight ratio of lipid/polymer that could achieve fulvestrant encapsulation above 80% was between the range of 20 to 30%. Above 30% weight ratio, PDI was much wider, particle size ranged more than 200 nm, and formulation showed two peaks of separate size distribution as seen in Figure 5.1. The two peaks were observed in the nanoparticles with lipid ratio of 35%, as the excess and unreacted lipids may have formed liposomes separately. The charge of nanoparticles with 35% lipids showed zeta potential of +49.1 mV suggesting the formation of separate liposomes (due to excessive lipids) which contributes to the more cationic charge in formulations.

Note: PLHNCs do not show zeta potential more than +30 mV due to charge balance between polymer and lipids. For further study, we optimized 25 % L/P ratio as further increasing L/P ratio showed no notable contribution in the encapsulation efficiency.

Table 5.4 Effect of L/P ratio on Fulvestrant encapsulation

Sr. No.	L/P Percentage ratio (%)	Mole Fraction (DOPE: SPC – 3: DSPE-PEG ₂₀₀₀)	Entrapment (%)	Size (nm)	PDI	Zeta Potential (mV)
1	5	30:50:20	51.3 \pm 1.8	96.5 \pm 3.4	0.135 \pm 0.011	-10.6 \pm 1.3
2	10	30:50:20	63.8 \pm 2.3	104.6 \pm 2.8	0.181 \pm 0.018	-4.7 \pm 0.8
3	15	30:50:20	71.6 \pm 2.8	110.7 \pm 3.1	0.241 \pm 0.021	3.5 \pm 0.6
4	20	30:50:20	85.2 \pm 3.5	99.8 \pm 1.6	0.049 \pm 0.007	11.3 \pm 1.1

5	25	30:50:20	87.6 ± 2.5	138.7 ± 2.2	0.327 ± 0.026	16.8 ± 1.6
6	30	30:50:20	88.1 ± 3.2	209.5 ± 6.3	0.428 ± 0.034	33.4 ± 2.1
7	35	30:50:20	89.6 ± 3.6	353.1 ± 2.9	0.676 ± 0.041	49.1 ± 3.2

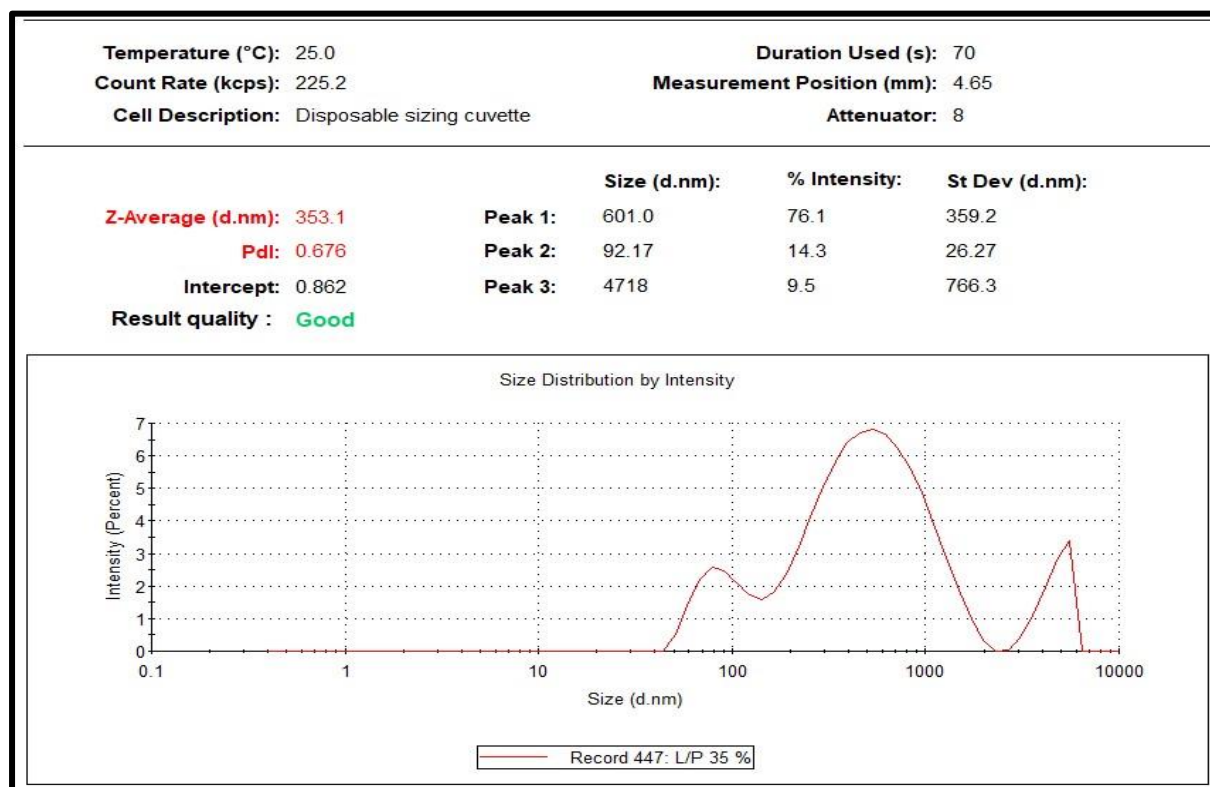


Figure 5.1 Particle Size distribution of L/P ratio 35%

5.3.6 Effect of drug input on encapsulation efficiency and particle size

As displayed in Table 5.5, as the initial drug input was increased more than 15%, encapsulation efficiency decreased and particle size increased. Increasing the drug concentration promotes the higher supersaturation that leads to a faster nucleation rate by promoting condensation and/or coagulation which results in increased particle size (12).

Table 5.5 Effect of fulvestrant input on encapsulation efficiency

Sr. No.	Drug input (%w/w of polymer)	Encapsulation Efficiency (%)	Size (nm)	Zeta Potential (mV)
1	10	86.1 ± 2.5	103.61 ± 2.5	27.1 ± 2.2
2	15	87.5 ± 3.1	169.24 ± 5.8	31.6 ± 1.9

3	20	74.6 ± 2.2	186.48 ± 3.7	23.4 ± 2.1
4	25	69.3 ± 1.8	268.32 ± 4.4	26.8 ± 1.7

5.3.7 Effect of number of extrusions on encapsulation and particle size

After evaporation of organic phase, the formulation was subjected to repetitive extrusion using laboratory manual extruder (Avastin LF-1) to optimize the encapsulation efficiency and particle size of the PLHNCs (Table 5.6).

Table 5.6 Effect of number of extrusions on encapsulation efficiency and particle size

Extrusion Cycles	Encapsulation efficiency (%)	Particle Size (nm)	PDI
2	78.24 ± 2.84	121.64 ± 2.5	0.346 ± 0.021
4	81.31 ± 3.18	114.23 ± 1.9	0.323 ± 0.013
6	82.43 ± 2.68	108.21 ± 1.4	0.312 ± 0.009
8	83.68 ± 3.24	104.63 ± 1.5	0.172 ± 0.008
10	85.18 ± 2.65	98.61 ± 1.2	0.049 ± 0.004
12	75.62 ± 3.84	112.25 ± 1.8	0.215 ± 0.011

For number of extrusions up to 10, there was significant improvement in PDI and particle size reduced, but as number of extrusions were increased, the particle size and PDI increased and encapsulation efficiency decreased due to excessive attrition force.

5.4 QUALITY BY DESIGN

To achieve the above quality profile, a systematic Quality by Design (QbD) method was used. A comprehensive QbD study should comprise of the following four key elements: (1) define target quality of product profile (goals) based on scientific foreknowledge and acceptable in vivo relevance; (2) design product and manufacturing techniques to gratify the pre-defined profile; (3) recognise critical quality attributes, processing parameters, and sources of variability to acquire the design space; and (4) control manufacturing techniques to generate consistent product quality over period through operating condition within the established design space (the margin of process and/or formulation variables that have been illustrated to provide assurance of quality), thus guaranteeing that quality is maintained into the product (ICH Q8). In addition, risk analysis narrowed down seven factors to elevated risk factors that

may influence the efficiency of PLHNCs drug encapsulation and particle size. For this purpose, two experimental designs were used (13). First, a Plackett–Burman screening design was used to identify the most significant factors affecting Fulvestrant encapsulation and particle size of developed PLHNCs. Next, a Box-Behnken (BBD) was used in the response surface study to obtain the exact relationship between the Fulvestrant encapsulation and various factors (that have been identified in the screening study). This model uses an articulated factorial design of centre points which is enhanced with a community of axial points that enables curvature calculation and allows the design to be rotatable (14). After obtaining the response surface, the optimal formulation and process conditions were identified. Further experimental tests were performed to test the robustness and accuracy of the generated model (15).

5.4.1 Plackett-Burman design for screening study (Primary design):

The results of preliminary studies were useful to identify formulation-related and process-related parameters and to understand the source of variables to improve the quality of product to assist formulation and process (16). Key product attributes recognized as particle size and encapsulation efficiency were evaluated for different variables. The goals of applying design were to achieve the highest encapsulation of Fulvestrant along with the lowest particle size and particle size distribution.

Table 5.7 Variables and levels selected for preliminary study

Factor	Name	Unit	Low actual	High actual
A	Polymer concentration	mg/mL	2	10
B	Lipid/Polymer ratio	%	5	35
C	Drug input	% w/w	5	20
D	Stirring speed	rpm	500	2000
E	Stirring time	H	0.5	4
F	Sonication time	s	20	100
G	No of Extrusion	-	2	10

The Plackett-Burman study design has been implemented for screening of various formulation and process-related parameters i.e., polymer concentration (mg/mL) (Factor A), lipid/polymer percentage (%) (Factor B), Drug input (% w/w) (Factor C), stirring speed (RPM)

(Factor D), stirring time (h) (Factor E), sonication time (S) (Factor F), no of extrusion (Factor G) (Table 5.8).

Table 5.8 Design Matrix of Plackett Burman Design

Run	Factor A Polymer Conc. (mg/mL)	Factor B L/P ratio	Factor C Drug input (% w/w)	Factor D Stirring speed (rpm)	Factor E Stirring Time (H)	Factor F Sonication Time (Sec)	Factor G No of Extrusion	Response -1 % EE (%)	Response -2 Particle Size (nm)
1	10	5	20	2000	0.50	100	10	65.48	142.36
2	2	5	5	2000	0.50	100	10	43.18	106.28
3	2	5	20	500	4	100	2	52.68	115.54
4	10	30	20	500	0.50	20	10	86.31	294.63
5	2	5	5	500	0.50	20	2	48.21	108.73
6	10	5	20	2000	4	20	2	65.69	156.87
7	2	30	20	2000	0.50	20	2	58.63	118.25
8	2	30	20	500	4	100	10	52.37	122.18
9	2	30	5	2000	4	20	10	54.32	102.24
10	10	5	5	500	4	20	10	56.84	165.31
11	10	30	5	2000	4	100	2	65.28	251.28
12	10	30	5	500	0.50	100	2	68.27	275.21

5.4.1.1 ANOVA for encapsulation efficiency (Factorial model)

Multi-linear regression analysis and ANOVA (Table 5.9) have been performed to analyse the data, and a series of Pareto charts were constructed to demonstrate the influence of each parameter on encapsulation efficiency.

Table 5.9 ANOVA on factorial model for encapsulation efficiency

Source	Sum of squares	Degree of Freedom	Mean square	F – Value	p-value (prob>F)
Model	1426.96	9	158.55	276.41	<0.0001
A: Polymer Conc.	775.66	1	775.66	1352.24	<0.0001
B-L/P	260.29	1	260.29	453.78	0.0022
C-Drug input	276.36	1	276.36	481.79	0.0021

D-Stirring Speed	1.06	1	1.06	1.85	0.3072
E-Stirring time	0.37	1	0.37	0.64	0.5077
F-Sonication time	129.12	1	129.12	225.11	0.0044
G-Number of Extrusions	16.70	1	16.70	29.11	0.0327
AB	86.24	1	86.24	150.35	0.0066
DG	29.36	1	29.36	51.18	0.0190
Model Statistics					
Standard Deviation			0.76		
Mean			59.77		
R ²			0.9992		
Adequate Precision			61.941		

The Model F-value of 276.41 implies the model is significant. There is only a 0.36% chance that a "Model F-Value" this large could occur due to noise. Values of "Prob > F" less than 0.0500 indicate model terms are significant. In this case A, B, C, F, G, AB, DG are significant model terms. Values greater than 0.1000 indicate the model terms are not significant. Adequate Precision measures the signal to noise ratio. A ratio greater than 4 is desirable. The ratio of 61.941 indicates an adequate signal. This model can be used to navigate the design space. Hence we can conclude that the polymer concentration (A), Lipid to polymer ratio (B) and Drug input (C), Sonication (F) and Number of Extrusions (G) are the potential factors that affect the encapsulation efficiency of the PLHNCs. Further there are significant interactions between Factor A and C whereas interactions between factor A & E and factor C & F are non-significant hence it has no impact on the encapsulation efficiency of PLHNCs (17).

5.4.1.2 Influence of factors on encapsulation efficiency (Pareto Chart)

The Pareto chart was used as a graphical tool to manage model selection for two-level factorial designs. As represented in Figure 5.3, as factor A (Polymer concentration) crossed the Bonferroni limit, it possesses the utmost importance for increasing encapsulation efficiency, while Factor B (L/P ratio) and C (Drug input) may have an intermediate effect on the encapsulation efficiency as they could cross the t-critical value limit. The t-critical value limit was considered as a lower limit for the factors that affect the response. Further, there were significant interactions between factor A & B and D & G, while interactions between factors

A & E and the factors C & F were not found significant, hence it had no impact on the encapsulation efficiency of PLHNCs.

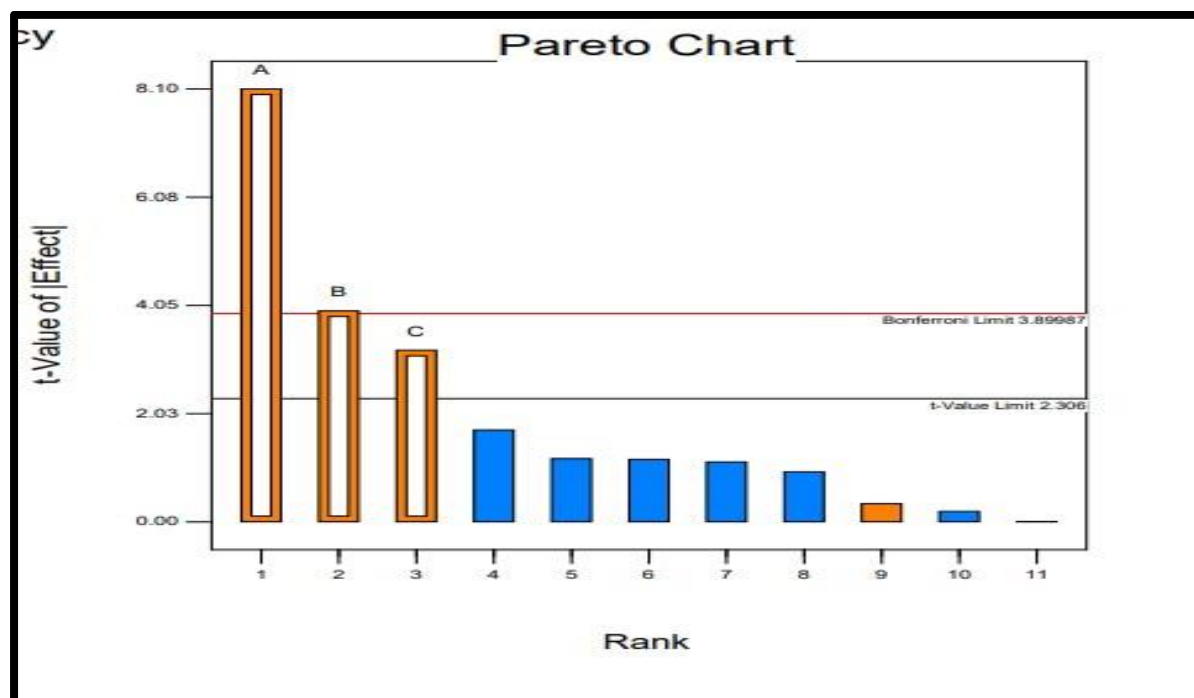


Figure 5.3 Pareto Chart for encapsulation efficiency

The Pareto chart depicted that the independent variables viz. concentration of polymer, lipid to polymer ratio and drug input have exerted most significant effect (Above t-value limit) on the response variables.

5.4.1.3 ANOVA for Particle Size (Factorial model)

Multi-linear regression analysis and ANOVA (Table 5.10) have been performed to analyse the data, and a series of Pareto charts were constructed to demonstrate the influence of each parameter on the particle size of PLHNCs.

Table 5.10 ANOVA on factorial model for particle size

Source	Sum of squares	Degree of Freedom	Mean square	F – Value	p-value (prob>F)
Model	53421.87	5	10684.37	117.92	< 0.0001
A-Polymer Conc.	31267.10	1	31267.10	345.10	< 0.0001
B-L/P	11334.45	1	11334.45	125.10	< 0.0001
C- Drug input	96.50	1	96.50	2.05	0.2265

D-Stirring Speed	647.82	1	647.82	7.15	0.0675
F-Sonication Time	180.12	1	180.12	3.82	0.1228
AB	7053.57	1	7053.57	77.85	0.0001
Model Statistics					
Standard Deviation			6.87		
Mean			163.26		
R ²			0.9965		
Adequate Precision			34.42		

The Model F-value of 117.92 implies the model is significant. There is only a 0.01% chance that a "Model F-Value" this large could occur due to noise. Values of "Prob > F" less than 0.0500 indicate model terms are significant. In this case A, B, D, AB are significant model terms. Values greater than 0.1000 indicate the model terms are not significant. The adequate precision of 34.423 indicates an adequate signal. This model can be used to navigate the design space. Hence, we can conclude that polymer concentration (A) and Lipid to polymer ratio (B) are the potential factors that affect the particle size of the PLHNCs and there is no cross-interaction between other factors that can lead to significant change in particle size of PLHNCs. Further, effect of two variables on particle size were screened using Box Behnken design.

5.4.1.4 Influence of factors on Particle Size (Pareto Chart)

As observed in Figure 5.4, factor A (polymer concentration) crossed the Bonferroni limit and possesses the utmost importance for increasing the particle size while factor B (L/P ratio) and D (stirring speed) may have an intermediate effect on the particle size since these factors could cross the t-critical value limit. In process parameters, stirring speed plays significant effect in governing particle size, as lower speed does not provide adequate shear and higher shear leads to vortex formation, providing inadequate mixing (18). Further, there was a significant interaction between A and B, but no significant interactions were found between any other factors.

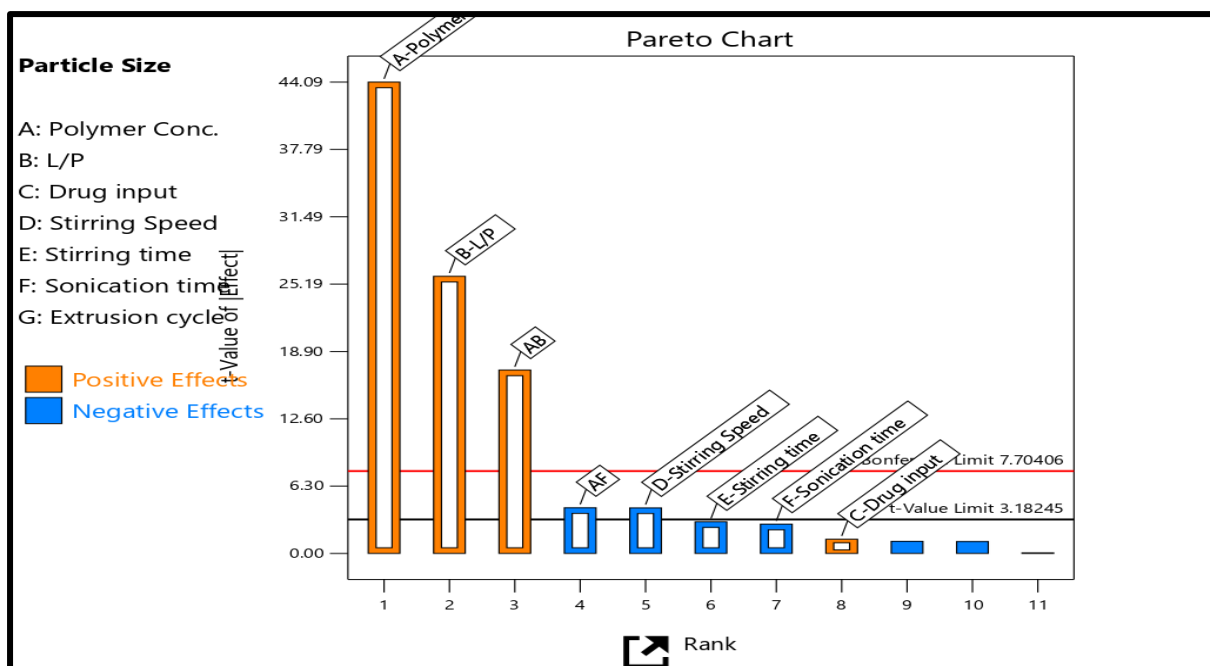


Figure 5.4 Pareto chart for particle size

The Pareto chart depicts that independent variables A (polymer concentration), B (lipid to polymer ratio) and D (stirring speed) have a significant impact on the particle size of the PLHNCs (above t-value limit).

5.4.2 Box Behnken design for point prediction (Secondary design)

Based on the results of the primary factor screening design, three variables, polymer concentration, lipid to polymer percentage and drug input were selected for further optimization using the response surface method, more specifically Box-Behnken design. The Box-Behnken design helps to analyse the influence of factors on characteristics of the PLHNCs. The three-factorial two-level Box-Behnken design, which consists of a set of points located at the midpoint of each end and the replicated central point of the multi-dimensional cube was used to obtain the polynomial models (19). A suitable design (Table 5.11) has been developed that integrates independent variables and generates the final equations that can result into a theoretical outcome for the response. The best suitable model has been selected for the point prediction and surface response curve for each response using ANOVA (20).

Table 5.11 Variables and levels selected based on PBD

Independent variables	Unit	Levels	
		-1	+1
A: Polymer concentration	mg/mL	4	12
B: Lipid to polymer ratio	%	10	30
C: Drug input	% w/w	5	15
Dependent variables	Unit		
1. Encapsulation Efficiency	Percentage		
2. Particle Size	Nm		

Table 5.12 Design matrix of Box -Behnken Design

Run	Factor A Polymer Concentration (mg/mL)	Factor B L/P ratio (%)	Drug input (w/w) (%)	Response – 1 Encapsulation Efficiency (%)	Response – 2 Particle Size (nm)
1	12	20	5	61.24	271.68
2	12	30	10	63.58	215.63
3	12	10	10	62.85	188.47
4	8	10	15	74.94	119.56
5	4	10	10	55.13	225.18
6	4	30	10	65.37	163.36
7	8	30	15	78.63	108.52
8	8	20	10	81.72	105.57
9	8	20	10	82.13	109.12
10	12	20	15	61.31	194.56
11	4	20	15	61.23	232.18
12	8	20	10	82.67	107.52
13	4	20	5	55.27	223.18
14	8	30	5	76.24	131.43
15	8	10	5	69.78	168.91

5.4.2.1 Statistical analysis of response: Encapsulation efficiency

5.4.2.1.1 ANOVA results of different models

Multi-linear regression analysis and ANOVA (Table 5.13) have been performed to analyse the data, and a series of response surface plots were constructed to demonstrate the influence of each parameter on encapsulation efficiency of PLHNCs.

Table 5.13 Summary of ANOVA results of different models for Encapsulation efficiency

Source	Sequential	Lack of fit	Adjusted	Predicted	Suggested model
	p-value	p-value	R-Squared	R-Squared	
Linear	0.8354	0.0016	-0.1810	-0.5902	
2FI	0.9855	0.0011	-0.5806	-2.1405	
Quadratic	<0.0001	0.6960	0.9983	0.9948	Suggested
Cubic	0.0020		0.9976		Aliased

Highest polynomial showing the lowest p value (<0.05) along with highest Lack of Fit p-value (>0.1) was considered for model selection. Based on the quality criteria, quadratic model was found to be best fitted to the observed responses. Special cubic and higher models were not suitable for prediction either due to low R-squared values and/or due to higher p value as compared to quadratic model (Table 5.14). Cubic model was aliased in the design as the number of points were very low to predict the responses to variables (21).

Table 5.14 ANOVA results of quadratic mixture model for encapsulation efficiency

Source	Sum of Squares	df	Mean Square	F – Value	p-value Prob > F	
Model	1341.71	9	149.08	899.46	< 0.0001	Significant
A – Polymer concentration	17.94	1	17.94	108.24	0.0001	
B – Lipid to polymer ratio	55.76	1	55.76	336.40	< 0.0001	
C – Drug input Percentage	23.05	1	23.05	139.08	< 0.0001	
AB	22.61	1	22.61	136.42	< 0.0001	

AC	8.67	1	8.67	52.33	0.0008	
BC	1.92	1	1.92	11.57	0.0192	
A²	1168.28	1	1168.28	7048.75	< 0.0001	
B²	25.99	1	25.99	156.79	< 0.0001	
C²	78.91	1	78.91	476.10	< 0.0001	
Residual	0.83	5	0.17			
Lack of fit	0.37	3	0.12	0.55	0.6960	Not significant
Pure Error	0.45	2	0.23			
Cor Total	1342.54	14				
ANOVA Summary						
Parameters	Results		Parameters		Results	
Std. Dev.	0.41		R – Squared		0.9994	
Mean	68.81		Adj. R – Squared		0.9983	
C.V %	0.59		Pred R – Squared		0.9948	
Press	7.02		Adeq. Precision		81.461	

The ANOVA table revealed that the effect of factors was significant and hence the model is significant for the Encapsulation Efficiency. The F-value was highest for the factor B (336.40), i.e., increasing lipid to polymer ratio would increase the entrapment of Fulvestrant in quadratic manner. Other two factors such as polymer concentration (factor A) and Drug input (factor C) have low effect on encapsulation efficiency compared to polymer concentration which can also be observed from the surface plots.

The Model F-value of 899.46 implies the model is significant. There is only a 0.01% chance that a "Model F-Value" this large could occur due to noise. Values of "Prob > F" less than 0.0500 indicate model terms are significant. In this case A, B, C, AB, AC, BC, A², B², C² are significant model terms. Values greater than 0.1000 indicate the model terms are not significant. The "Lack of Fit F-value" of 0.55 implies the Lack of Fit is not significant relative to the pure error. There is a 69.60% chance that a "Lack of Fit F-value" this large could occur due to noise. The "Pred R-Squared" of 0.9948 is in reasonable agreement with the "Adj R-Squared" of 0.9983. The adequate precision of 81.461 indicates an adequate signal. This model can be used to navigate the design space.

5.4.2.1.2 Model diagnostic plots for encapsulation efficiency

5.4.2.1.2.1 Normal residual plot

The normal probability plot (normal plot of residuals) shows whether the residuals follow a normal distribution or not and helps identify any specific patterns in the residuals indicative of requirement of transformations i.e., “S-shaped” curve, etc. the normal plot of residuals for the current data follows a straight line, indicating no abnormalities. For design to be normal, it is not mandatory for the data to follow straight line. A good rule of thumb is called the “fat pencil” test. If you can put a fat pencil over the line and cover up all the data points, the data is sufficiently normal. In this case, the plot looks to fit in fat pencil form (Figure 5.5). Hence plot is considered as normal (22).

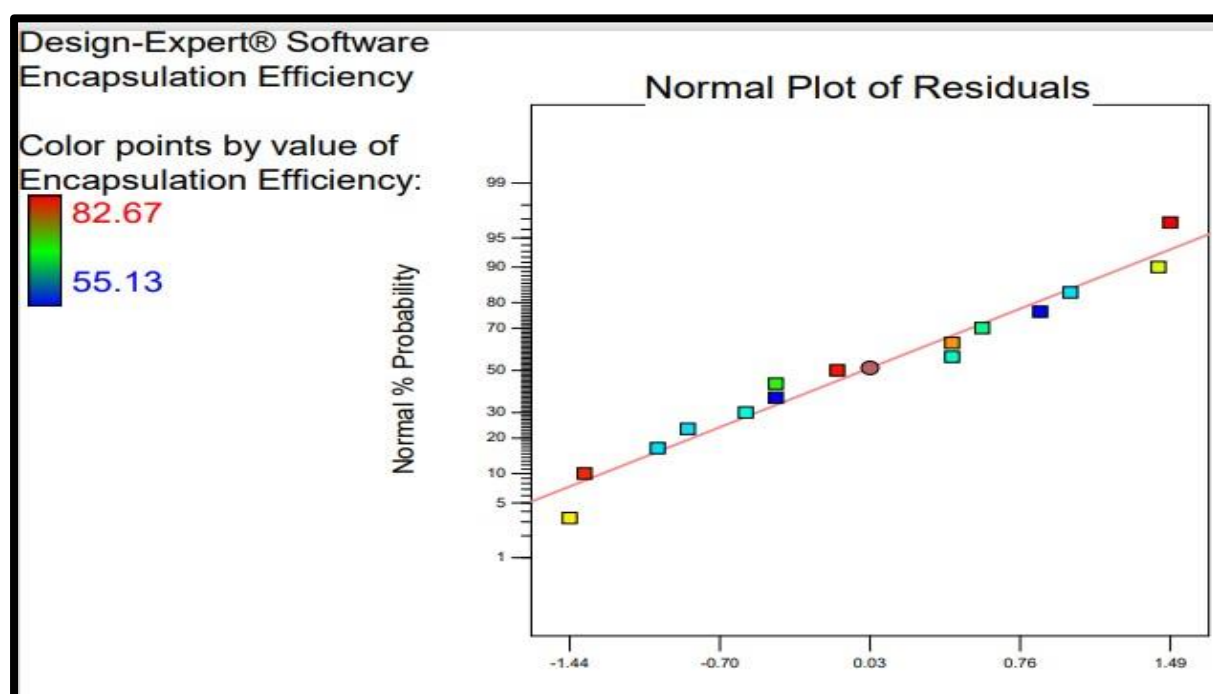


Figure 5.5 Normal plot of residuals for encapsulation efficiency

5.4.2.1.2.2 Residuals vs predicted plot

Residuals vs. predicted response (ascending values) plot tests if variance is distributed over the design constantly i.e., variance is not associated with the factor values as megaphone patterns (pattern like sign horizontal cone $>$ or $<$) which indicate either decreasing or increasing residuals with increasing the factor values. The size of the residual should be independent of its predicted value. Figure 5.6 shows absence of horizontal cone type pattern that indicates distribution of variance all over the design space (23).

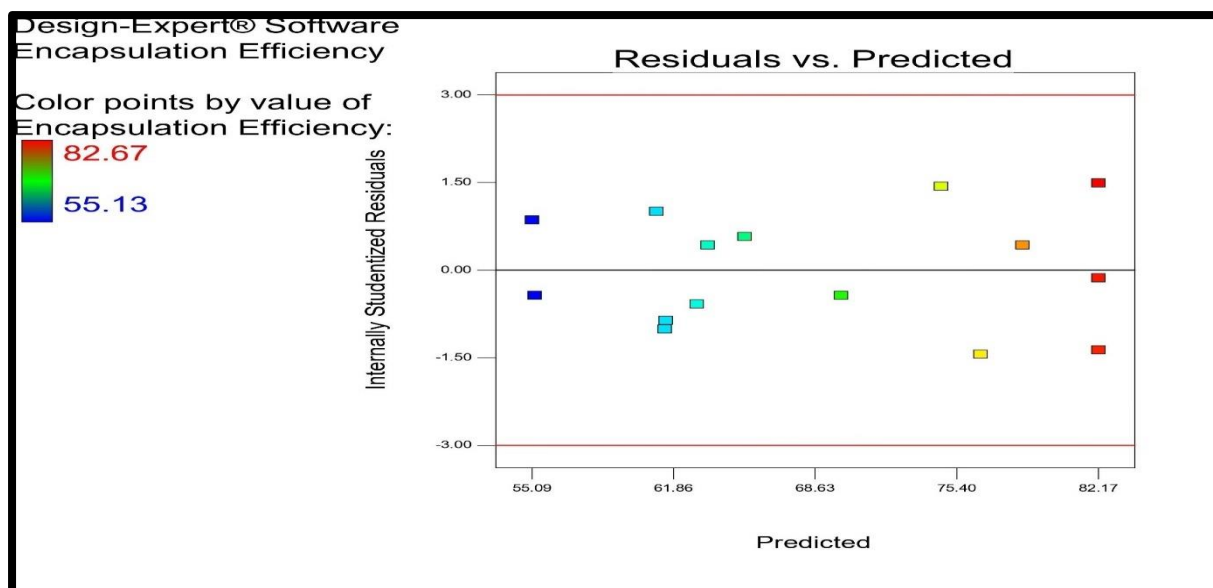


Figure 5.6 Residual vs. Predicted plot for encapsulation efficiency

5.4.2.1.2.3 Residual vs. Run order plot

Residual vs Run plot for order of experiments explains the randomization in experiment. Figure 5.7 shows a random scatter of residuals which indicates the absence of time dependent changes and continuous downward or upward trend was also not observed. Hence it was confirmed that experimental runs were in random manner and selected model did not generate any biased result in the design and point prediction (24).

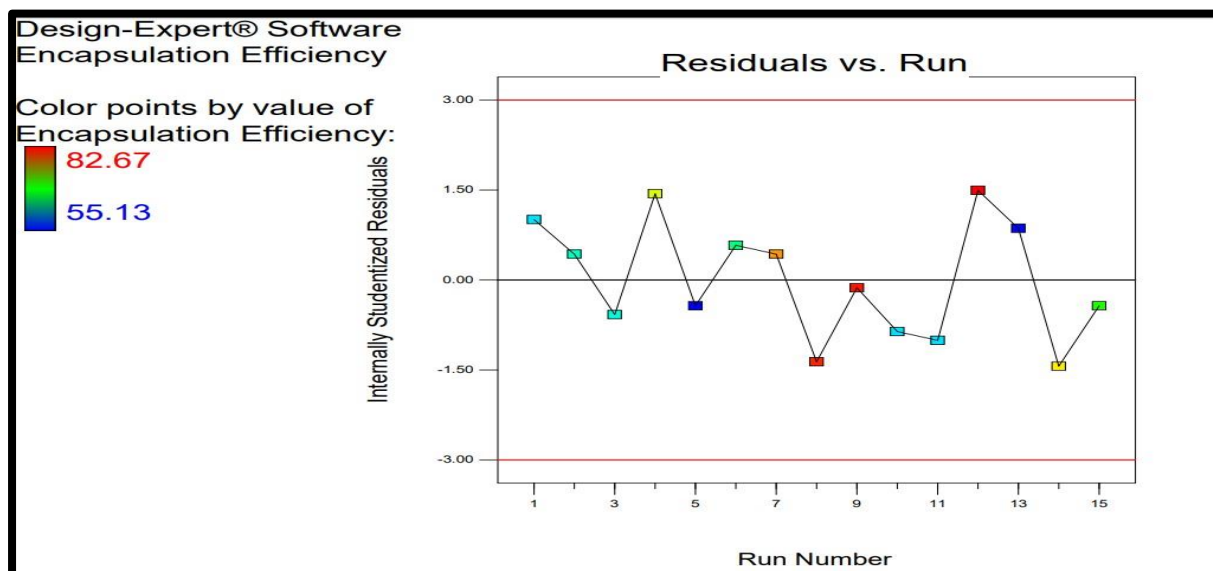


Figure 5.7 Residual vs. Run plot for encapsulation efficiency

5.4.2.1.2.4 Predicted vs. Actual plot

Plot from data shows (Figure 5.8) a straight line at 45° that indicates that model selected for prediction of response fits overall design matrix.

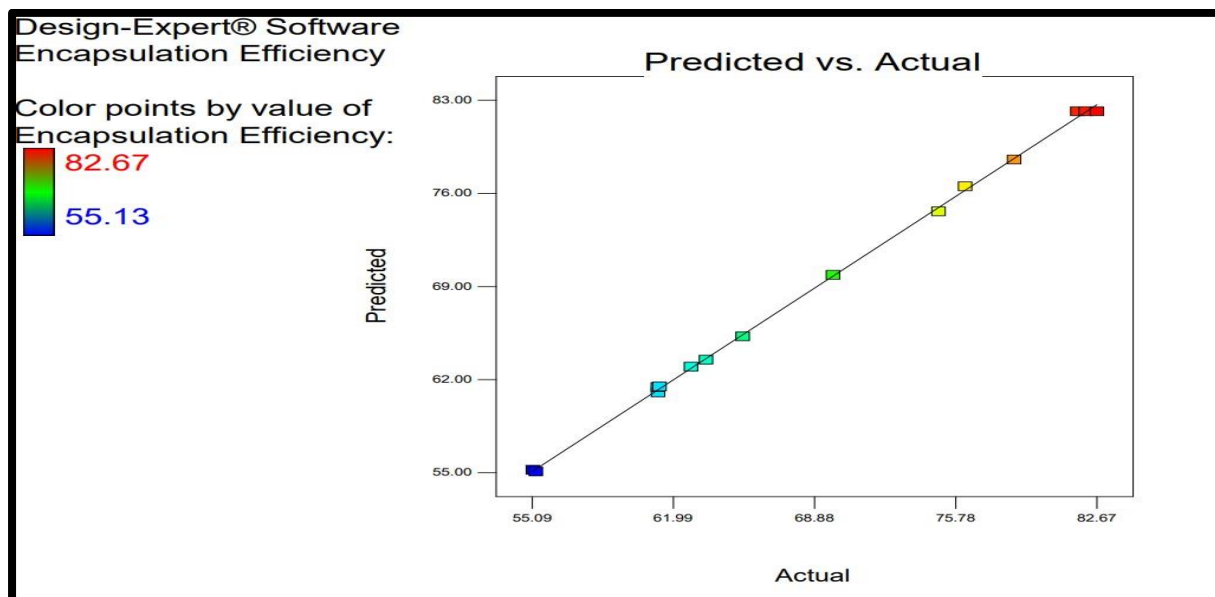


Figure 5.8 Predicted vs. Actual plot for the encapsulation efficiency

5.5.2.1.2.5 Box-Cox plot for power transformation

Box-Cox plot of Ln (residuals sum of squares) vs. λ for power transformation helps to select any power transformation of observed response values required for fitting the model based on the best λ value and 95% confidence interval around it. Plot in Figure 5.9 shows the λ value of 1, which lies near the best λ value and within 95% confidence interval of the design (25).

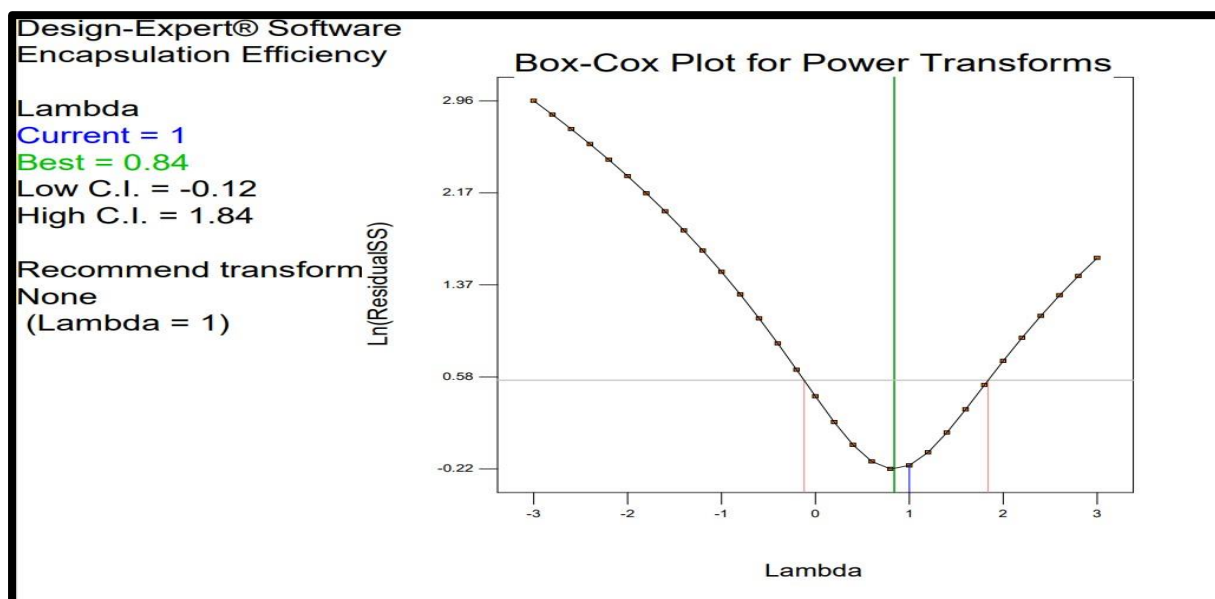


Figure 5.9 Box-Cox plot for power transformation for the encapsulation efficiency

5.5.2.1.2.6 Piepel's plot

Piepel's plot is a trace plot showing the effect of individual factors plotting the pseudo limits of one component keeping the ratio of the changeable amounts of each component constant against the response. The responses are plotted as deviations from the reference blend i.e., centroid (pseudo center point of the constrained design). A steep slope for factor A (Concentration of polymer) and curvature for factor B and C (Lipid to polymer percentage ratio and Drug input respectively) as shown in Figure 5.10 proves that the response is sensitive to factor. The line for the polymer concentration shows sharp steep which suggests that concentration of polymer has a great impact on the encapsulation efficiency (26).

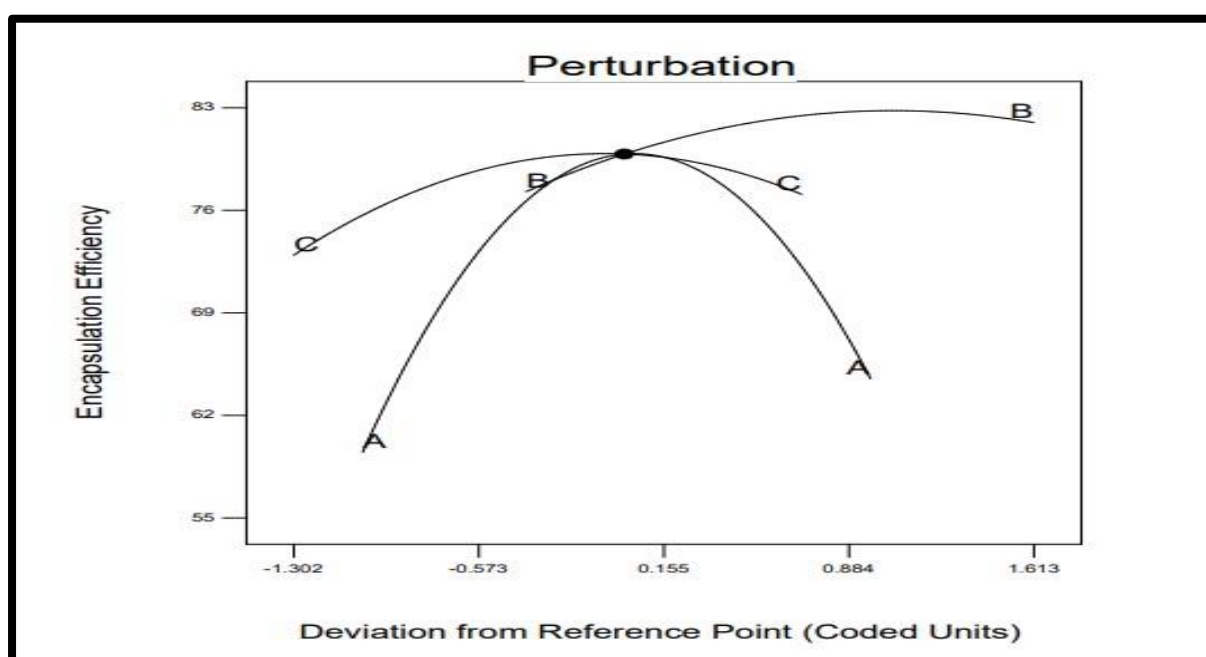


Figure 5.10 Piepel's plot

5.5.2.1.2.7 Response surface (3D) plots

The value of ANOVA gives us idea about the factors having significant effect on Encapsulation Efficiency which is shown in contour and 3D plots. The RED area in the Figure 5.11 shows the area of maximum Encapsulation Efficiency and BLUE zone represents the area with lowest Encapsulation Efficiency(27).

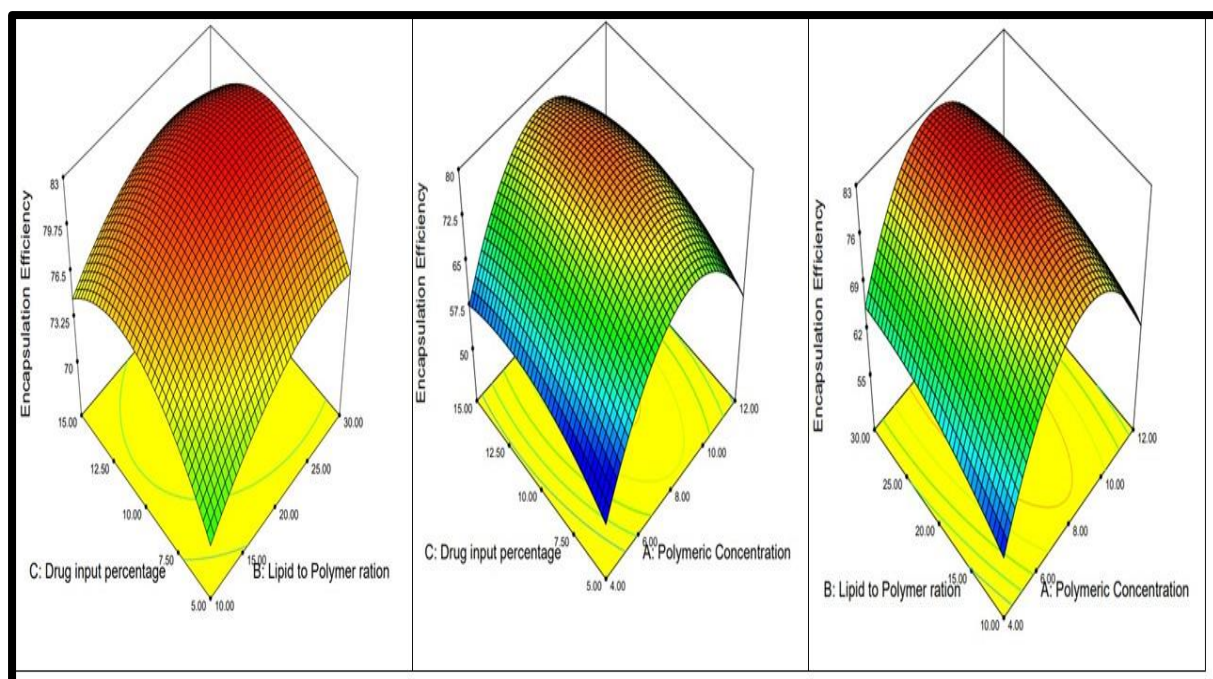


Figure 5.11 Effects of various factors on FLV entrapment by 3D surface curve

Two-factor 3D response surface plots for fulvestrant entrapment justifies the effect of aforementioned significant terms. From the plots, it is concluded that increasing the concentration of fulvestrant and polymer initially increases the FLV encapsulation but after a certain saturation concentration, the encapsulation efficiency goes down. This may be due to the limited loading capacity in polymer matrix and lipid layer. All response surface (3D) plots show combined effect of concentration of polymer, lipid to polymer percentage and drug input on % Encapsulation Efficiency. From the graph, increase in the Encapsulation Efficiency were noticed with increasing concentration of polymer and lipid to polymer ratio. Though polymer concentration had great impact on the encapsulation efficiency, outer lipid also played an important role in improving the encapsulation efficiency. The lipid plays important role in coating on the surface of polymer and acts as surfactant during encapsulation.

5.4.2.1.3 Mathematical equation for Encapsulation Efficiency

Final equation in terms of coded factors has been obtained as below:

$$\text{Encapsulation efficiency} = +82.17 + 1.50*A + 2.64*B + 1.70*C - 2.38*A*B - 1.47*A*C - 0.69*B*C - 17.79*A^2 - 2.65*B^2 - 4.62*C^2. \text{----- (5.1)}$$

5.4.2.2 Statistical analysis of response: Particle size

5.4.2.2.1 ANOVA results of different models

Multi-linear regression analysis and ANOVA (Table 5.15) have been performed to analyse the data, and a series of response surface plots were constructed to demonstrate the influence of each parameter on particle size of PLHNCs.

Table 5.15 Summary of ANOVA results of different models for particle size

Source	Sequential	Lack of fit	Adjusted	Predicted	Suggested Model
	p-value	p-value	R-Squared	R-Squared	
Linear	0.8117	0.0007	-0.1709	-0.6879	
2FI	0.9306	0.0005	-0.4458	-2.2126	
Quadratic	<0.0001	0.2568	0.9977	0.9888	Suggested
Cubic	0.0009	0.1103	0.9908		Aliased

Highest polynomial showing the lowest p value (<0.05) along with highest Lack of Fit p-value (>0.1) was considered for model selection. Based on the quality criteria, quadratic model was found to be best fitted to the observed responses. Special cubic and higher models were not suitable for prediction either due to low R-squared values and/or due to higher p value as compared to quadratic model (Table 5.16). Cubic model was aliased in the design as the number of points are too low to predict the responses to variables

Table 5.16 ANOVA results of quadratic mixture model for particle size

Source	Sum of Squares	df	Mean Square	F – Value	p-value Prob > F	
Model	42672.85	9	4741.43	673.22	< 0.0001	Significant
A – Polymer concentration	87.38	1	87.38	12.41	0.0169	
B – Lipid to polymer ratio	864.86	1	864.86	122.80	0.0001	
C – Drug input Percentage	2463.32	1	2463.32	349.76	< 0.0001	
AB	1979.36	1	1979.36	281.04	< 0.0001	
AC	1854.16	1	1854.16	263.27	< 0.0001	
BC	174.77	1	174.77	24.81	0.0042	
A²	32991.26	1	32991.26	4684.35	< 0.0001	

B²	52.46	1	52.46	7.45	0.0413	
C²	2992.94	1	2992.94	424.96	< 0.0001	
Residual	35.21	5	7.04			
Lack of fit	28.89	3	9.63	3.05	0.2568	Not significant
Pure Error	6.32	2	3.16			
Cor Total	42708.07	14				
ANOVA Summary						
Parameters	Results		Parameters		Results	
Std. Dev.	2.65		R – Squared		0.9992	
Mean	170.99		Adj. R – Squared		0.9977	
C.V %	1.55		Pred R – Squared		0.9888	
Press	476.51		Adeq. Precision		76.322	

The ANOVA table revealed that the effect of factors was significant and hence the model was significant for the particle size. The F value was the highest for the factor C (349.76), i.e., increasing the Drug input decreased the particle size in quadratic manner. Lipid to polymer ratio and drug input have most prominent effect as their p-value is <0.0001. With increasing the lipid to polymer ratio, the lipid provided the surfactant effect, encapsulated more drug in the matrix and lowered the particle size.

The Model F-value of 673.22 implies the model is significant. There is only a 0.01% chance that a "Model F-Value" this large could occur due to noise. The "Lack of Fit F-value" of 3.05 implies the Lack of Fit is not significant relative to the pure error. There is a 25.68% chance that a "Lack of Fit F-value" this large could occur due to noise. The "Pred R-Squared" of 0.9888 is in reasonable agreement with the "Adj R-Squared" of 0.9977. Adequate Precision" measures the signal to noise ratio. A ratio greater than 4 is desirable. The ratio of 76.322 indicates an adequate signal.

5.4.2.2.2 Model diagnostic plots for Particle Size

5.4.2.2.2.1 Normal residual plots

The normal probability plot (normal plot of residuals) which shows whether the residuals follow a normal distribution or not and helps identify any specific patterns in the residuals indicative of requirement of transformations i.e., "S-shaped" curve, etc. The normal plot of residuals for the current data follows a straight line, indicating no abnormalities. The more the

data is near the line, more will be the linearity. As per the normal probability curve rule, data should be in 95 % CI range (Figure 5.12) and the responses obtained were following the same.

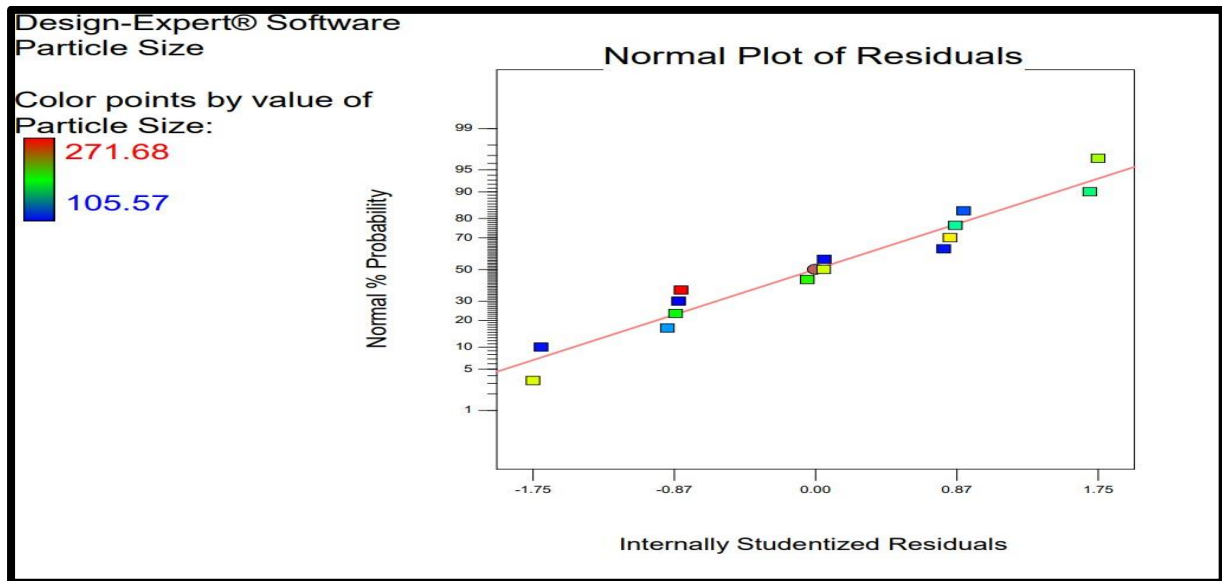


Figure 5.12 Normal plot of residuals for particle size

5.4.2.2.2 Residuals vs Predicted plot

The responses in Figure 5.13 showed the distribution of variance throughout the design space and it did not follow any specific pattern indicating the random distribution of variance and randomization of predicted value to residual values.

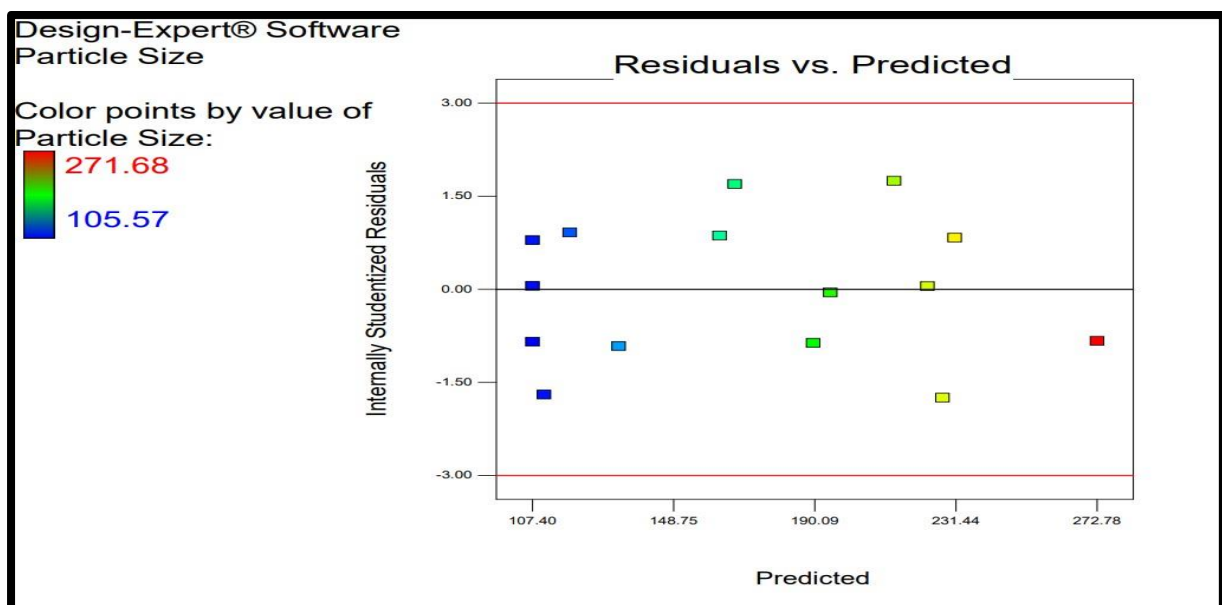


Figure 5.13 Residual vs. Predicted plot for particle size

5.4.2.2.3 Residual vs. Run plot

The residual vs run data for particle size (Figure 5.14) is having a random scatter of residuals which indicate there is no time dependent changes occurring in the residuals. The points plotted in random plot doesn't follow a fixed pattern of runs, which explains the randomization of design carried out for identification of independent variables on dependent responses.

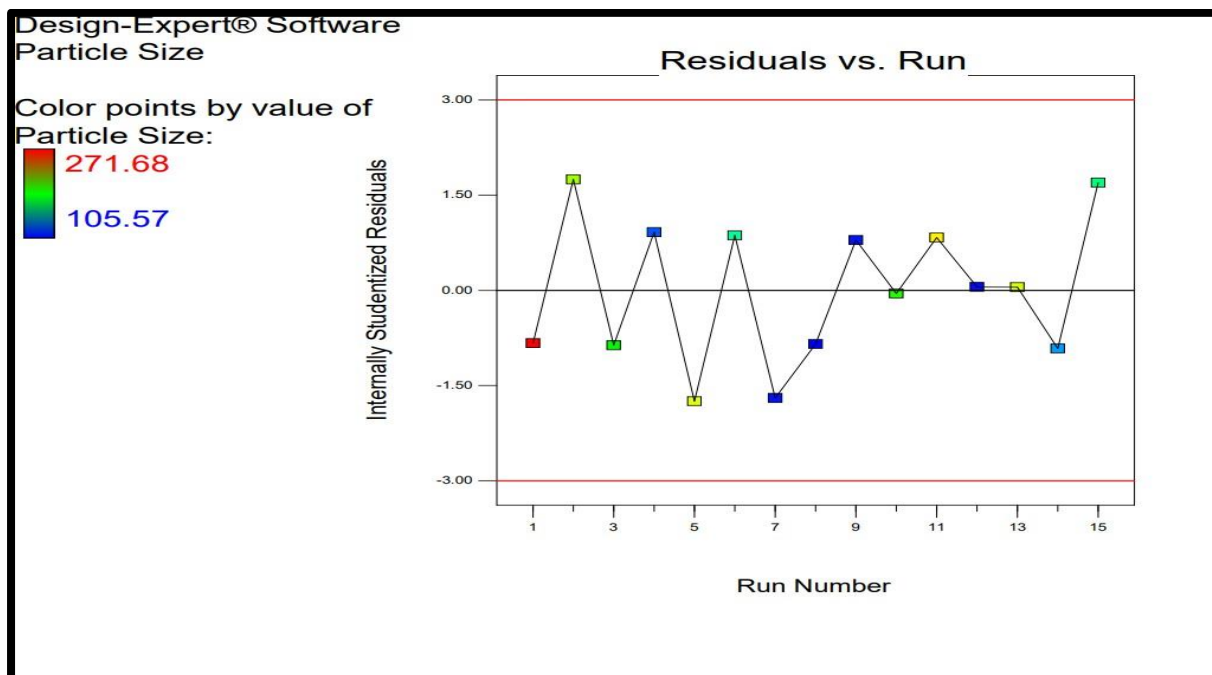


Figure 5.14 Residual vs Run Plot for particle size

5.5.2.2.4 Predicted vs. Actual plot

The actual points followed an angle of 45° (Figure 5.15) and none of the point was found to deviate from linearity, so the plot of predicted vs actual points proved the data to be free from error as well as bias.

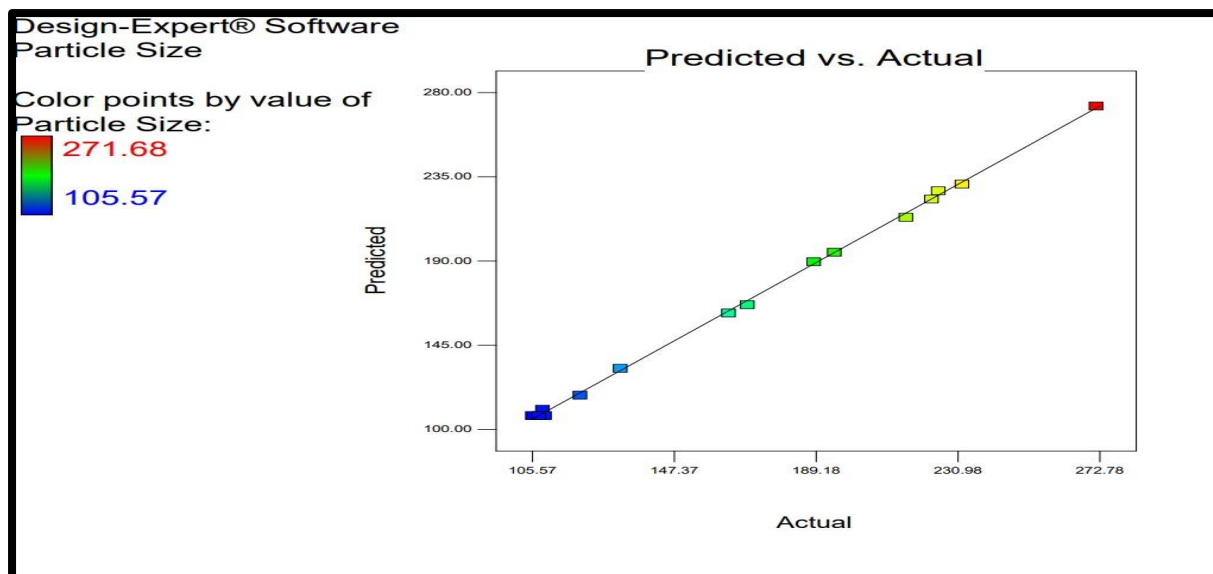


Figure 5.15 Predicted vs Actual plot for particle size

5.4.2.2.5 Box cox plot for power transformation

The box plot for transformation showed the value near to 1 and the range of CI was between 0.86 to 1.56. The observed values indicated that the design data followed the criteria of 95% CI (Figure 5.16).

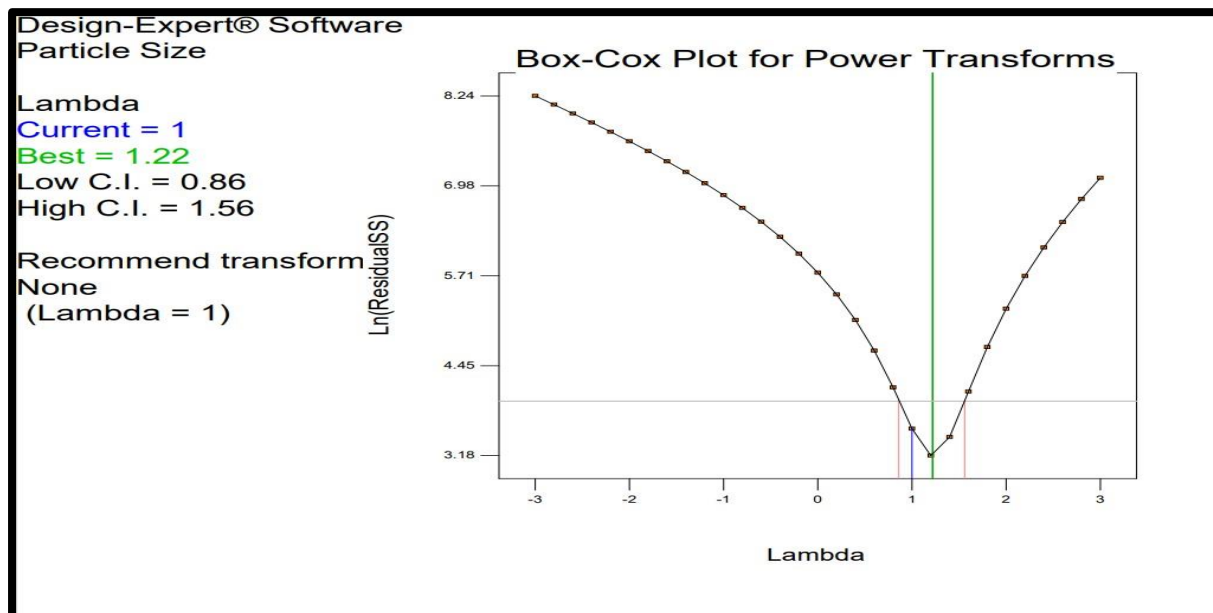


Figure 5.16 Box cox plot for power transformation for the particle size

5.4.2.2.6 Piepel's plot

A curvature for factor A, slope for factor C and straight line for factor B (Figure 5.17) proved that the response was sensitive to the factors. The factor with slope had most significant effect

on the response and factor with straight line had least impact on the response. Polymer concentration (factor A) and drug input (factor C) had most significant effect, whereas lipid to polymer ratio has the least significant effect on particle size.

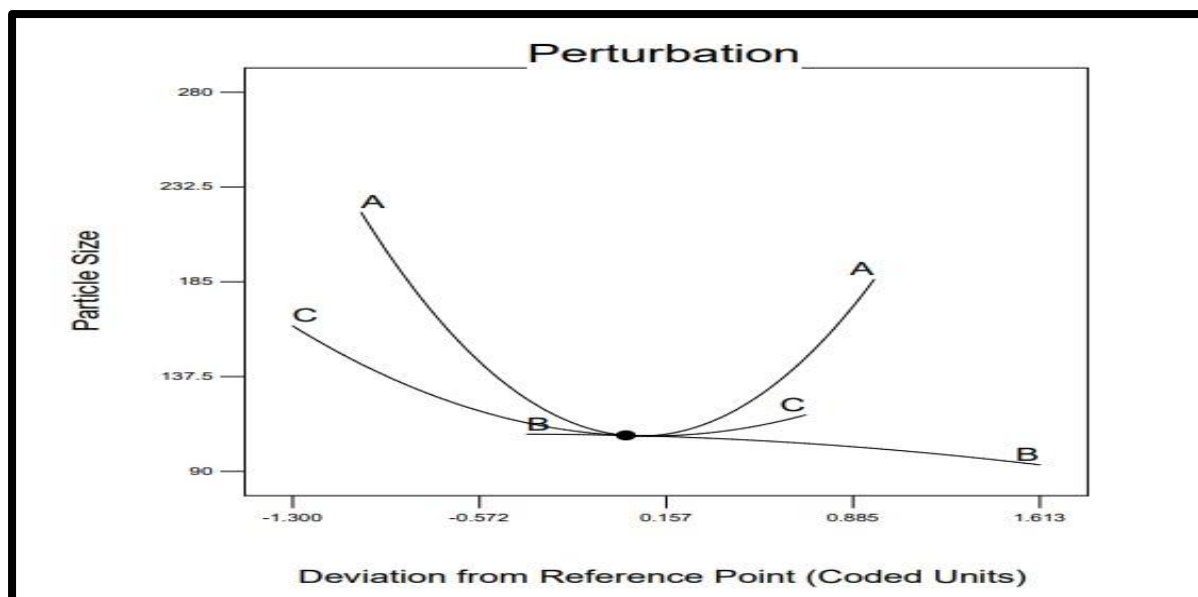


Figure 5.17 Piepel's plot for particle size

5.4.2.2.7 Response surface (3D) plots

The value of ANOVA gives us idea about the factors having significant effect on particle size which is shown in contour and 3D plots. The RED area in the Figure 5.18 shows the area of maximum particle size and BLUE zone represents the area with lowest particle size.

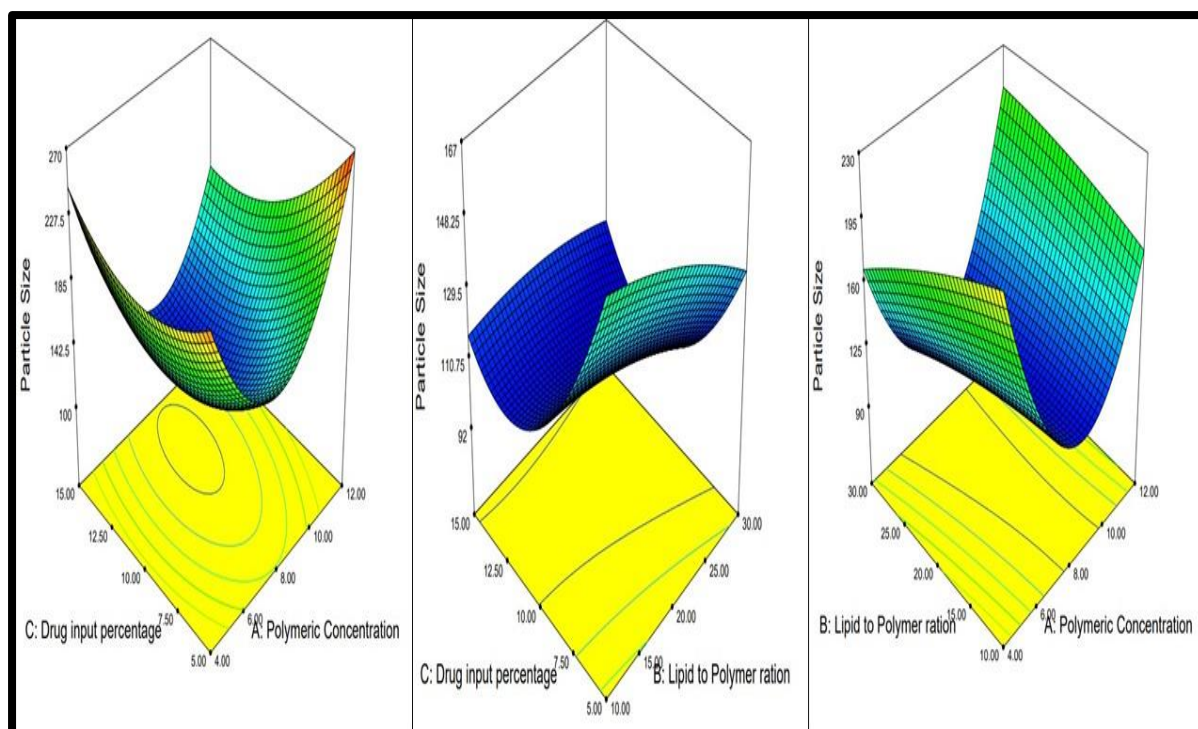


Figure 5.18 Effects of various factors on PLHNCs particle size by 3D Surface plots

As per the ANOVA data, all the three independent variables have significant effect on the particle size based on its p-value, i.e., $p < 0.05$. From the plots, it can be concluded that on increasing the polymer concentration and Drug input, the entrapment increases but there was no significant effect on its particle size due to phase saturation, but with further increase in polymer concentration and drug input, there was a significant increase in the particle size, due to increase in the overall viscosity of the system and supersaturation of drug suspension that leads to faster nucleation rate by promoting condensation and/or coagulation which results in increased particle size.

5.4.2.2.3 Mathematical equation for particle size

$$\text{Particle Size} = +107.40 + 3.30*A - 10.40*B - 17.55*C + 22.25*A*B - 21.53*A*C + 6.61*B*C + 94.53*A^2 - 3.77*B^2 + 28.47*C^2 \text{ ----- (5.2)}$$

5.4.3 Desirability plot and overlay plot for optimization

Desirability plot was generated using Design Expert 7.0. Parameters for the desirability batch are shown in Table 5.17.

Table 5.17 Variable for desirability plot and goals for response

Name	Goal	Lower Limit	Upper Limit
A: Polymer Concentration (mg/mL)	In range	4	12
B: Lipid to Polymer percentage	In range	10	30
C: Drug input percentage	In range	5	15
Quality Target			
Encapsulation Efficiency (%)	Maximize	75	85
Particle Size (nm)	Minimize	95	130

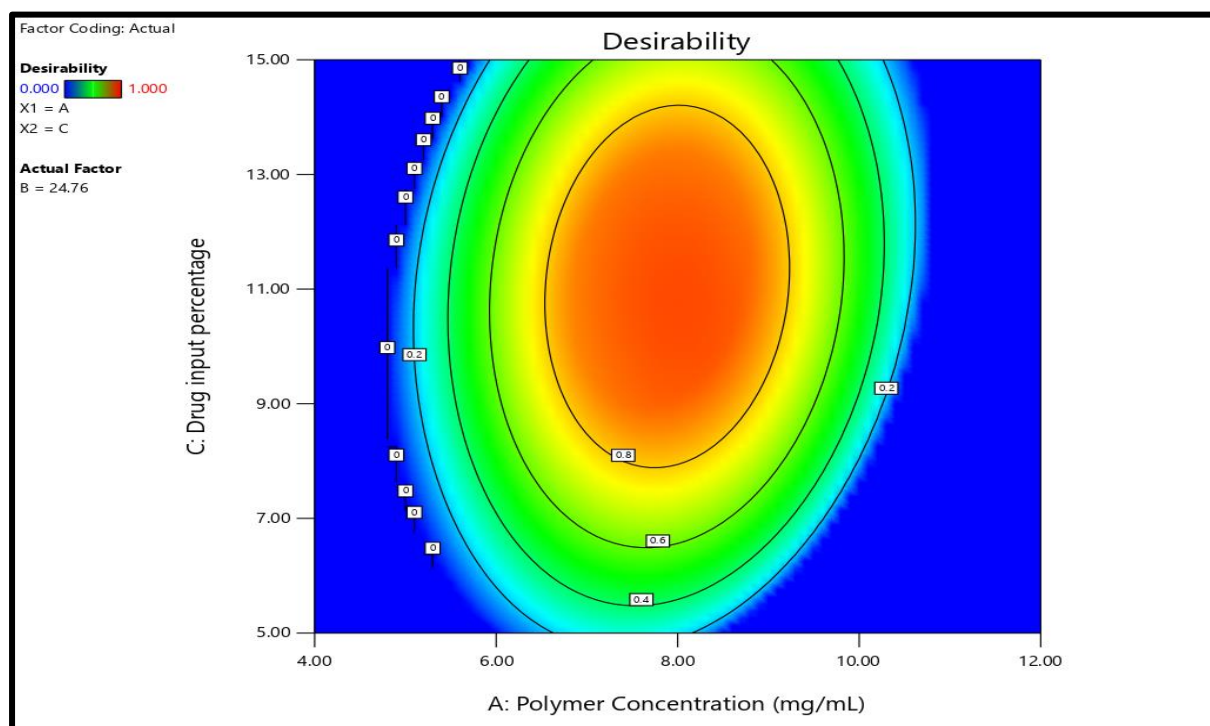


Figure 5.19 Desirability plot

5.4.4 Point prediction and confirmation

From the Box-Behnken design, three most desirable batches were selected for further optimization and lyophilization. Confirmation of the responses was done by carrying out the experiment using selected factor values in triplicate. (Table 5.18)

Table 5.18 Process parameters for optimized batch

Variables	Predicted Values	Actual values
A: Polymer Concentration (mg/mL)	8.02	8.00
B: Lipid to Polymer ratio	24.76	25.00
Drug input (%)	10.74	11.00

Table 5.19 Predicted vs Actual Experimental results

Batch No.	Parameters	Predicted values	Observed Values	%Error
1.	Encapsulation Efficiency (%)	82.93	82.13 ± 2.52	0.96
2.	Particle Size (nm)	100.14	101.9 ± 3.8	1.75

5.5 CHARACTERIZATION

5.5.1 Determination of encapsulation efficiency of Fulvestrant

The exact amount of fulvestrant incorporated in PLHNCs was identified by the RP – HPLC method. Briefly, specified amount of lyophilized nanocarriers were suspended in 10 mL mixture of acetonitrile, methanol, and water (6.5:1.5:2) and sonicated for 3 minutes to disrupt the polymer and lipid layers. 1 mL of PLHNCs suspension was diluted in acetonitrile to make the final volume up to 5 mL and further diluted with methanol up to 10 mL. The above mixture was then vortexed for 1 min. and centrifuged at 10,000 rpm for 15 minutes. From the supernant, aliquot was withdrawn and 20 µL of sample was injected into the RP – HPLC system. Estimation of fulvestrant content in PLHNCs was performed by RP – HPLC (Vanquish Core, Thermo Scientific) using C18 ODS Hypersil Gold Column (250 mm x 4.6 mm, 5µ, Thermo Scientific) at 35°C. The mobile phase Methanol:Water:ACN (65:20:15) was allowed to run at a flow rate of 1 mL/min, Diode array detector, at wavelength of 280 nm.

$$\% \text{ encapsulation efficiency} = \frac{\text{Amount of drug entrapped}}{\text{Total amount of drug}} \times 100 \text{ --- (5.3)}$$

5.5.2 Phospholipid content by Stewart method

Total phospholipid content was measured in the PLHNCs formulation by following the procedure described in Chapter 4.

5.5.3 In-vitro drug release study and drug release kinetics

The in vitro drug release study and drug release kinetics were determined as per the procedure described in Chapter 3, Section 3.2.5.

5.5.4 Estimation of residual solvent by Gas Chromatography

Standard Preparation: The typical acetonitrile assay was carried out by taking 100 μ l of acetonitrile in a 10 ml volumetric flask and adjusting the level with DMF so that the final concentration will be 10,000 ppm. Take 1 ml in a 10 ml volumetric flask from the above solution and deionized water was used to make up the mark, so the concentration was 100 ppm.

Sample Preparation: 100 μ l of PLHNCs formulation was taken in 10 ml volumetric flask and diluted up to mark using DMF. From the above solution, 1ml was taken and added to 5ml volumetric flask to make up the volume using Deionized water.

5.6 RESULTS AND DISCUSSION

5.6.1 Particle size distribution by dynamic light scattering (DLS)

The nanocarrier size obtained in the present study (Figure 5.20) was 101.9 ± 3.8 nm , with a low polydispersity index of 0.133 ± 0.014 .

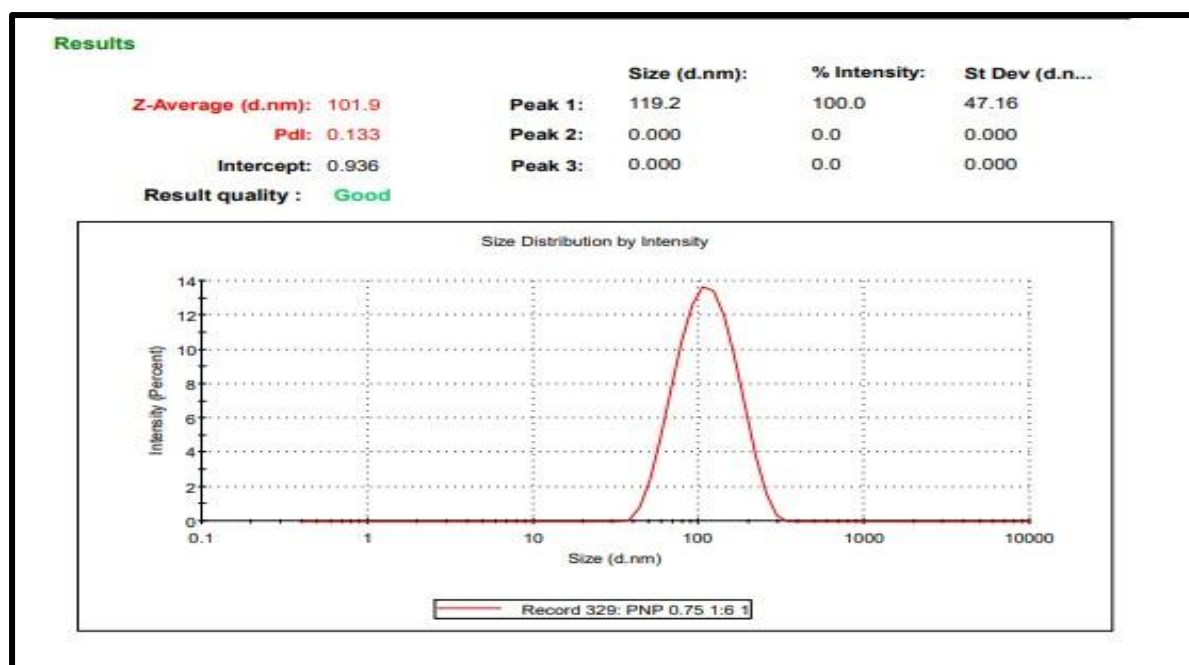


Figure 5.20 Particle size and PDI of optimized PLHNCs batch

Nanocarrier size is significant property, as it can affect the biopharmaceutical properties of the PLHNCs. The biodistribution of particulate matter can also depend on the size of the particle and particle endocytosis is also dependent on size. Another size-dependent phenomenon was stated to be particle uptake, where the small particles could be picked up effectively relative to the larger particles. Particle size is important for cancer cells to target the EPR (Enhanced Permeability and Retention) effect, which plays a very critical role in targeting (28).

5.6.2 Zeta Potential of optimized PLHNCs

The zeta potential of PLHNCs was found to be $+28.3 \text{ mV} \pm 1.28$ as shown in Figure 5.21. Positive zeta potential of PLHNCs was due to presence of DOPE on outer lipid layer. Positively charged PLHNCs particles will repel each other and account for stability by preventing aggregation. Moreover, cationic charge of PLHNC is advisable for higher cellular uptake (29).

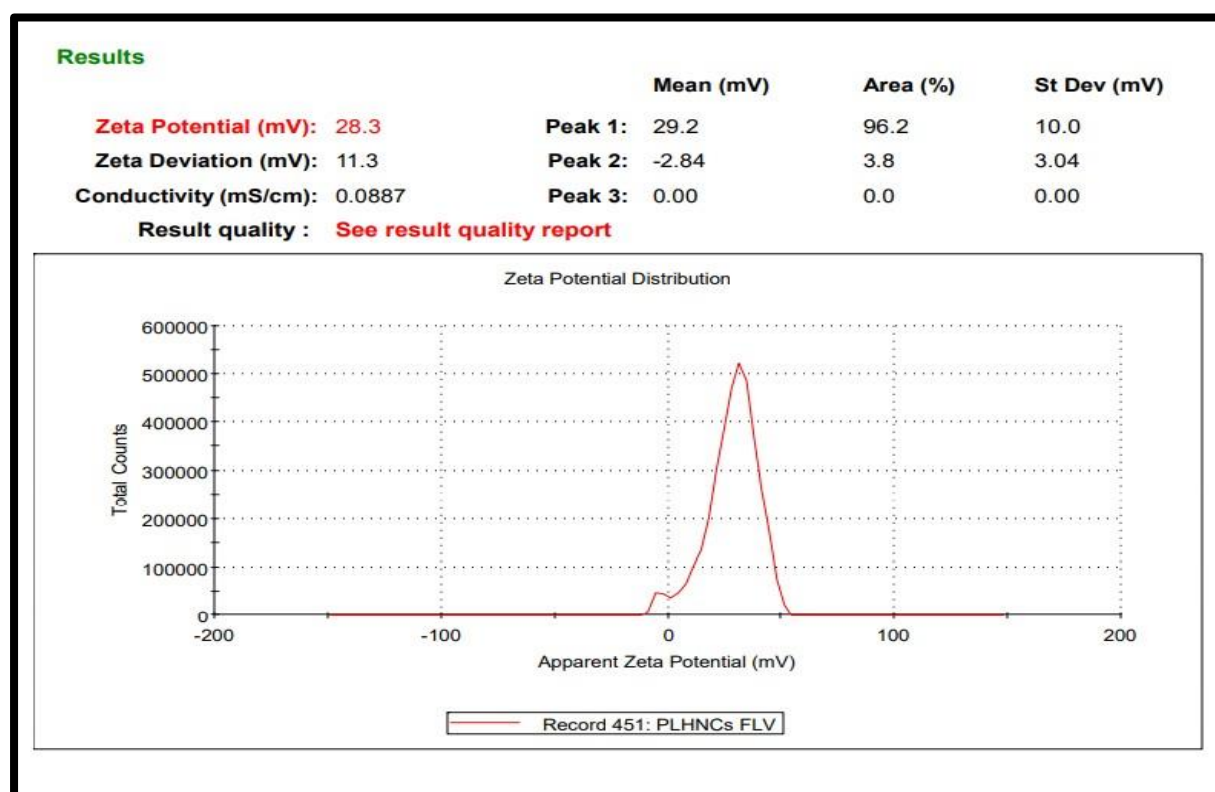


Figure 5.21 Zeta potential of optimized PLHNCs

5.6.3 Estimation of total phospholipid content

The total amount of phospholipid present in the nanoparticulate formulation was calculated by the steward method. The volume based calculation was carried out on the dry weight basis between the amount added and amount observed after nanoparticle formation.

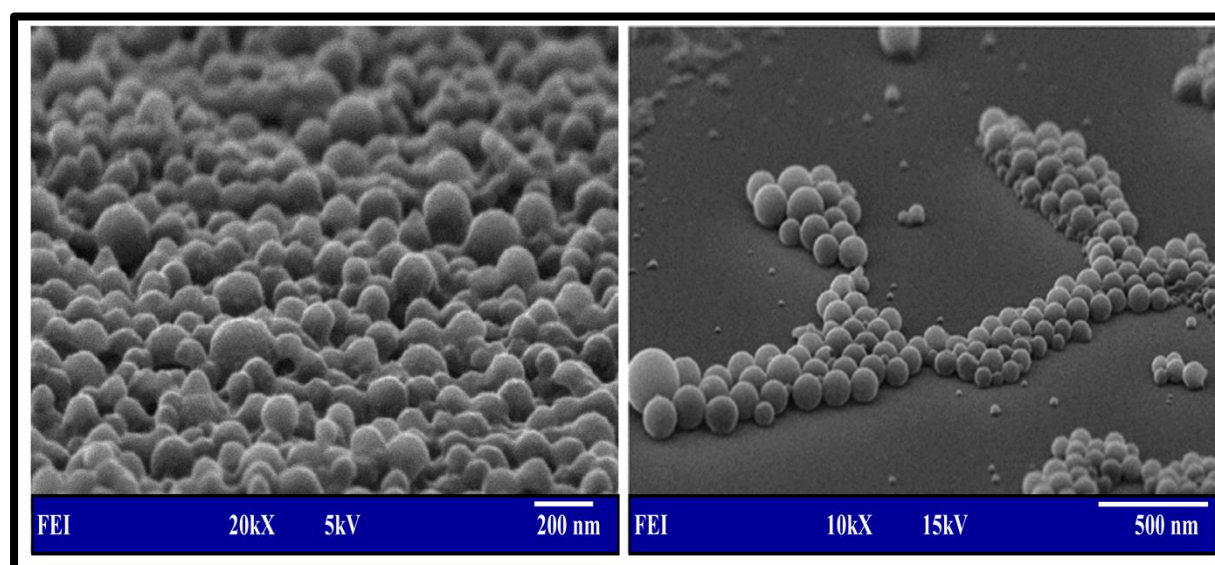
Table 5.20 Total Phospholipid content present in optimized batch

Batch Volume	Theoretical amount of phospholipid	Observed amount of phospholipid	Assay (%)
10 ml	20 mg	18.64 ± 2.16 mg	93.20
25 ml	50 mg	46.32 ± 5.28 mg	92.64
50 ml	100 mg	91.36 ± 8.62 mg	91.36

The amount of phospholipid has been found to be similar to of theoretical phospholipid content, which suggested absence of any reaction between phosphate group of lipids in the formulation, and lipid layer remained intact on the polymeric surface.

5.6.4 Scanning Electron Microscopy (SEM) Analysis

The shape and surface morphology of prepared nanocarriers were confirmed with the help of FEG-SEM. The shape of nanocarrier was found to be spherical and the particles were found to have smooth texture (Figure 5.22). The particle size of nanocarriers was found to be 121.4 nm.

**Figure 5.22 SEM images of optimized PLHNCs**

5.6.5 Transmission Electron Microscopy (TEM)

Negative staining with uranyl acetate in TEM was conducted for structural characterization of PLHNCs, which stains the lipid layer that was observed as a dim ring circling the polymeric centre (Figure 5.23). The ring diameter was less than 20 nm which confirms the morphology

and architecture of PLHNCs. The negative stain separates the positively charged lipid from the polymer layer.

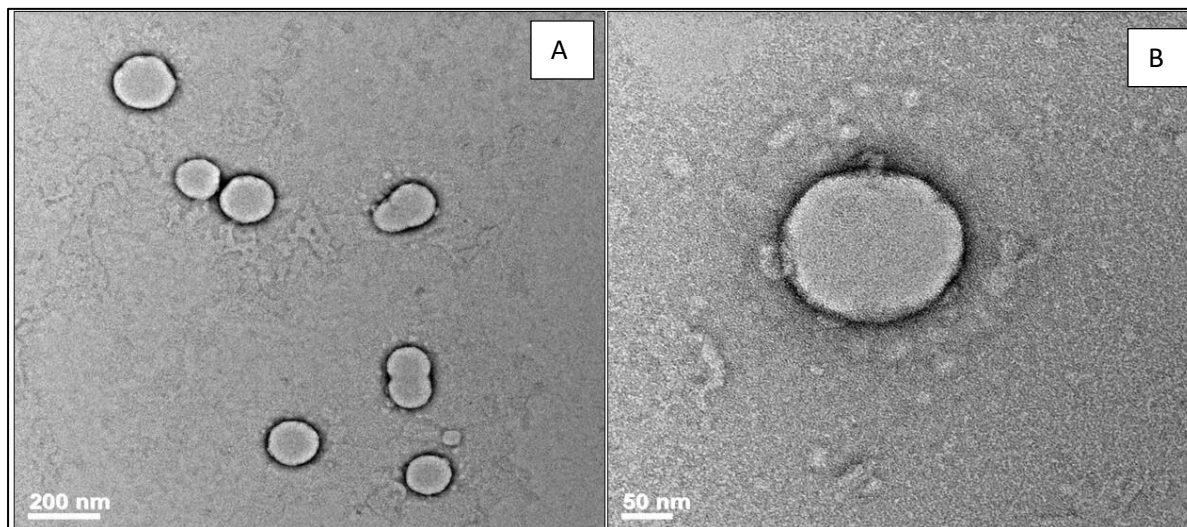


Figure 5.23 (A) Nanoparticle suspension (B) Representative nanoparticle showing separate ring stained by Uranyl acetate

5.6.6 In-vitro drug release study and drug release kinetics

Fulvestrant loaded PLHNCs followed the sustained release kinetics (Figure 5.24). From the three pH conditions, maximum drug release was found in pH 5.5, which suggested maximum release of the drug in cancer cells. Release of fulvestrant from the PLHNCs in the different media was observed to be in decreasing order of pH 5.5 > pH 6.6 > pH 7.4, which indicates least drug release in plasma and blood due to presence of DOPE, a pH dependent lipid coat which disintegrates below the pH 6.

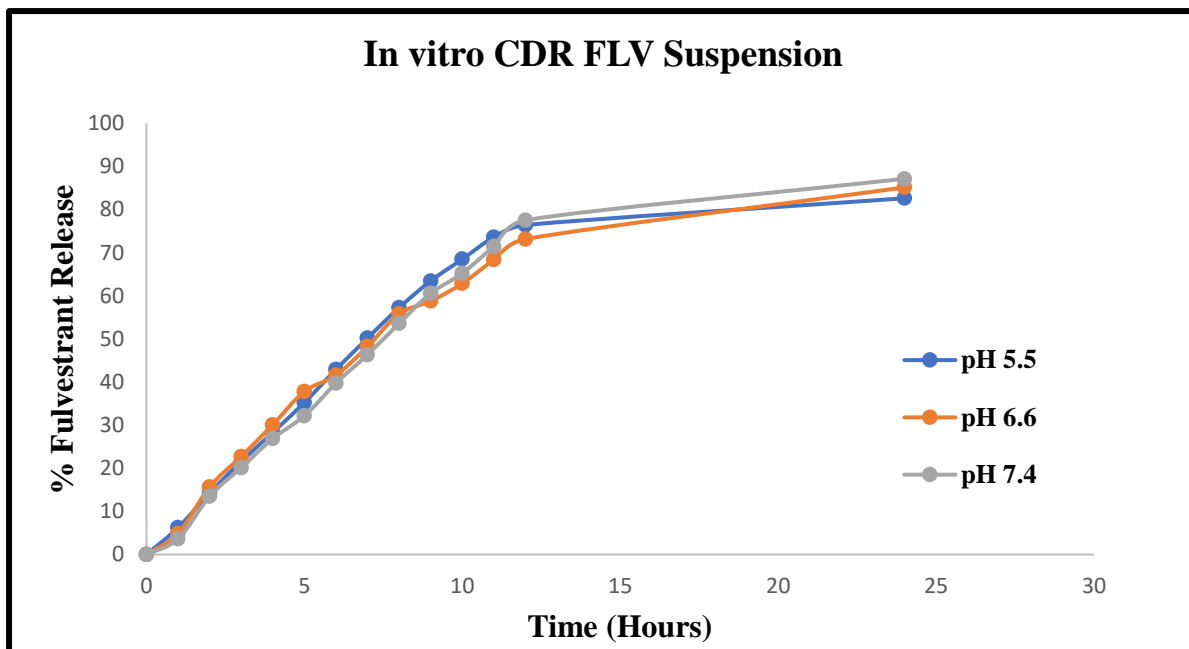


Figure 5.24 In vitro drug release of fulvestrant suspension

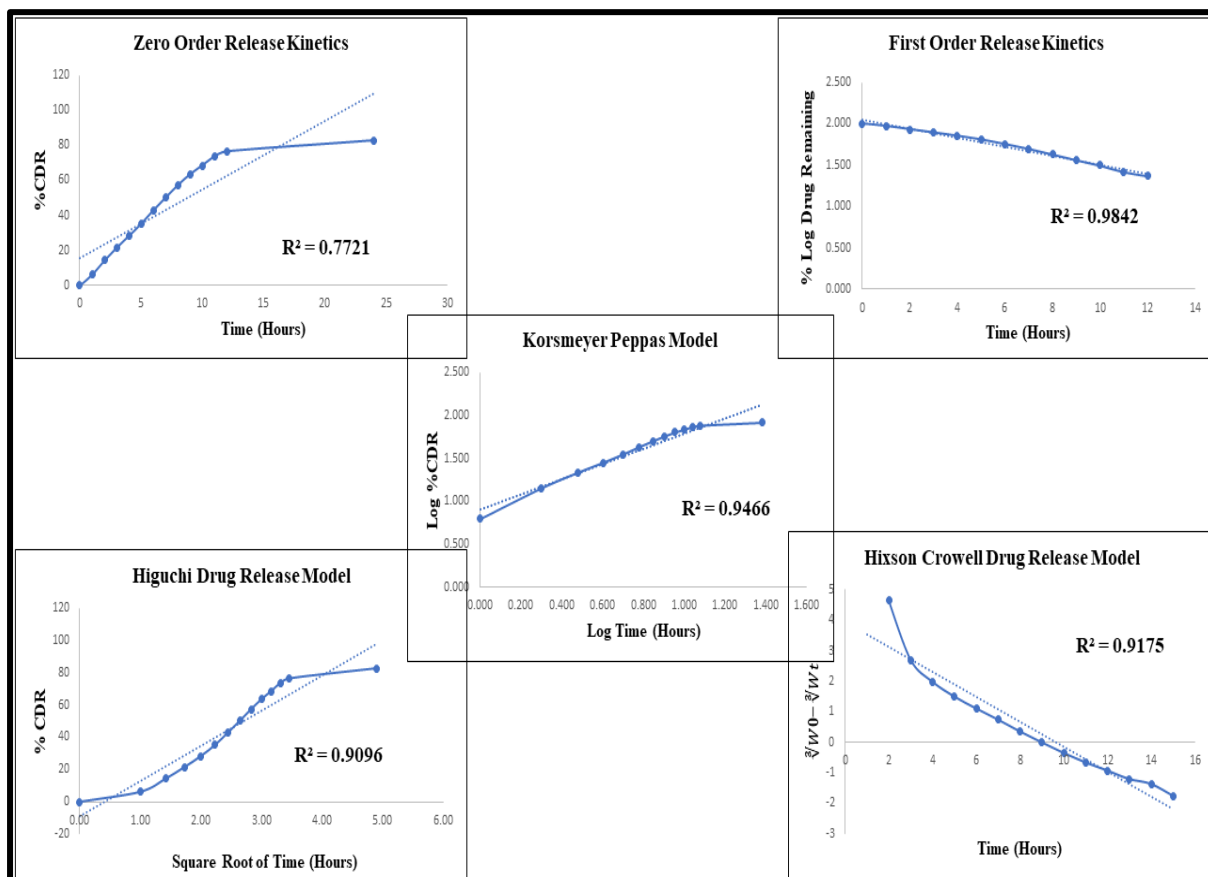


Figure 5.25 Drug release kinetics for FLV Suspension pH 5.5

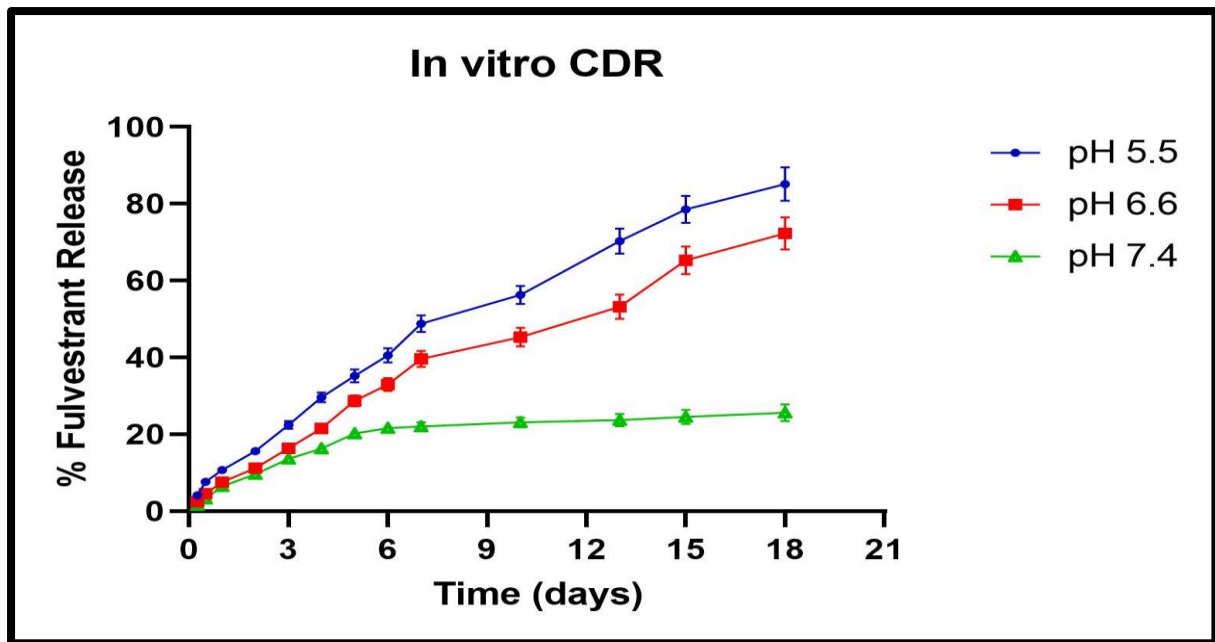


Figure 5.26 In vitro drug release of FA FLV PLHNCs

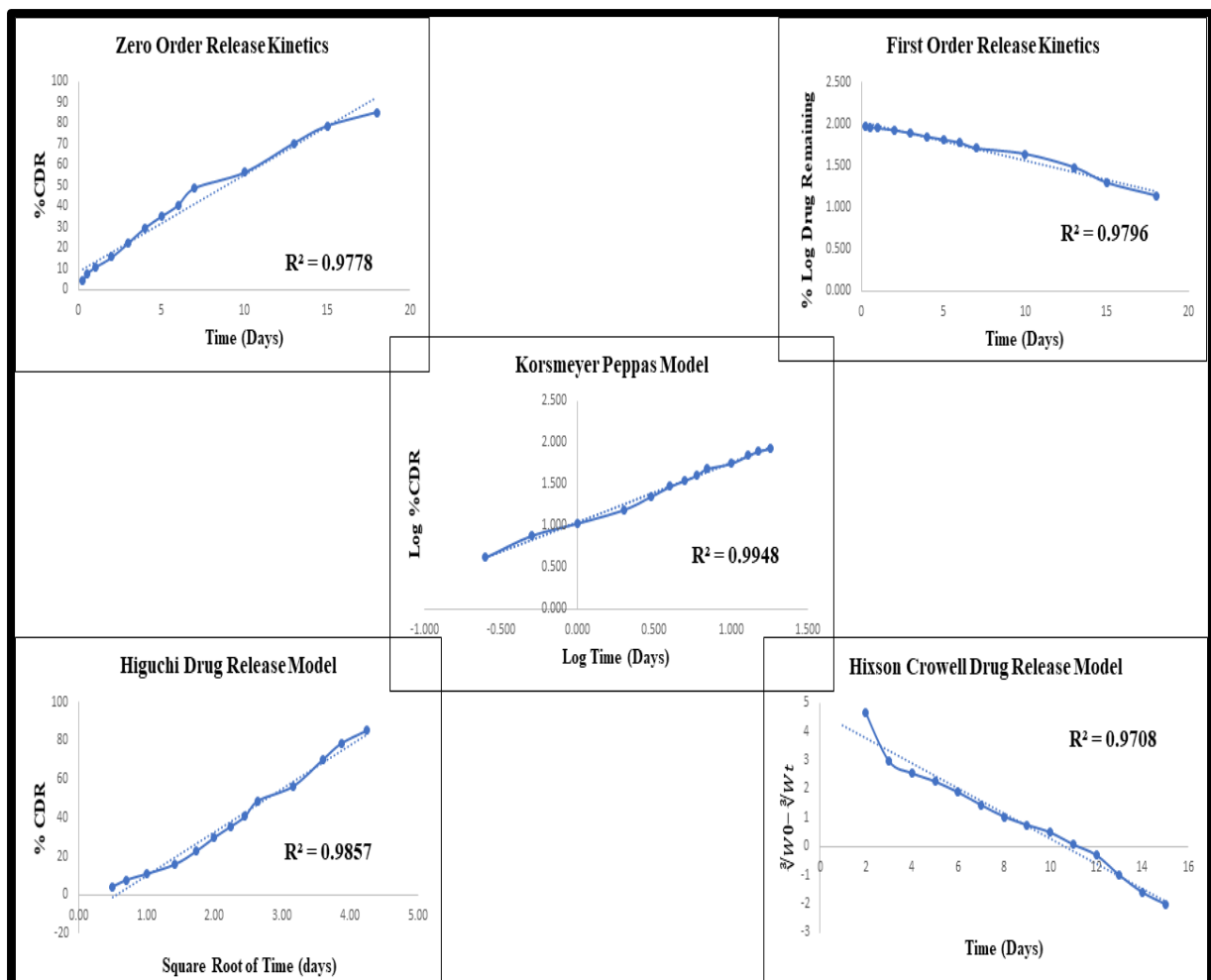


Figure 5.27 Drug release kinetics for FA FLV PLHNCs pH 5.5

From the kinetic model fitting analysis, it was concluded that for fulvestrant suspension followed First order release kinetics whereas, fulvestrant loaded PLHNCs, followed Korsmeyer Peppas model (Figure 5.27) with R^2 value of 0.9948, with the n value of 0.711, which is consistent with the drug release by anomalous transport or non-Fickian diffusion that involves two phenomena: drug diffusion and relaxation of the polymer matrix. The comparison of models are shown in Table 5.21.

Table 5.21 Drug release kinetics for fulvestrant formulations

Model	FA FLV PLHNCs	FLV Suspension
Zero Order	0.9778	0.7721
First Order	0.9796	0.9842
Higuchi	0.9857	0.9096
Korsmeyer Peppas	0.9948	0.9466
Hixson Crowell	0.9708	0.9175

5.6.7 Estimation of residual solvent by Gas Chromatography

As per the ICH guidelines Q3C (R6), acetonitrile is CLASS II solvent and the permitted daily exposure limit is 4.1 mg/day which is equivalent to 410 ppm per day exposure. Figure 5.26(a) shows GC chromatograph for standard acetonitrile solution and (b) shows the GC chromatograph for PLHNCs

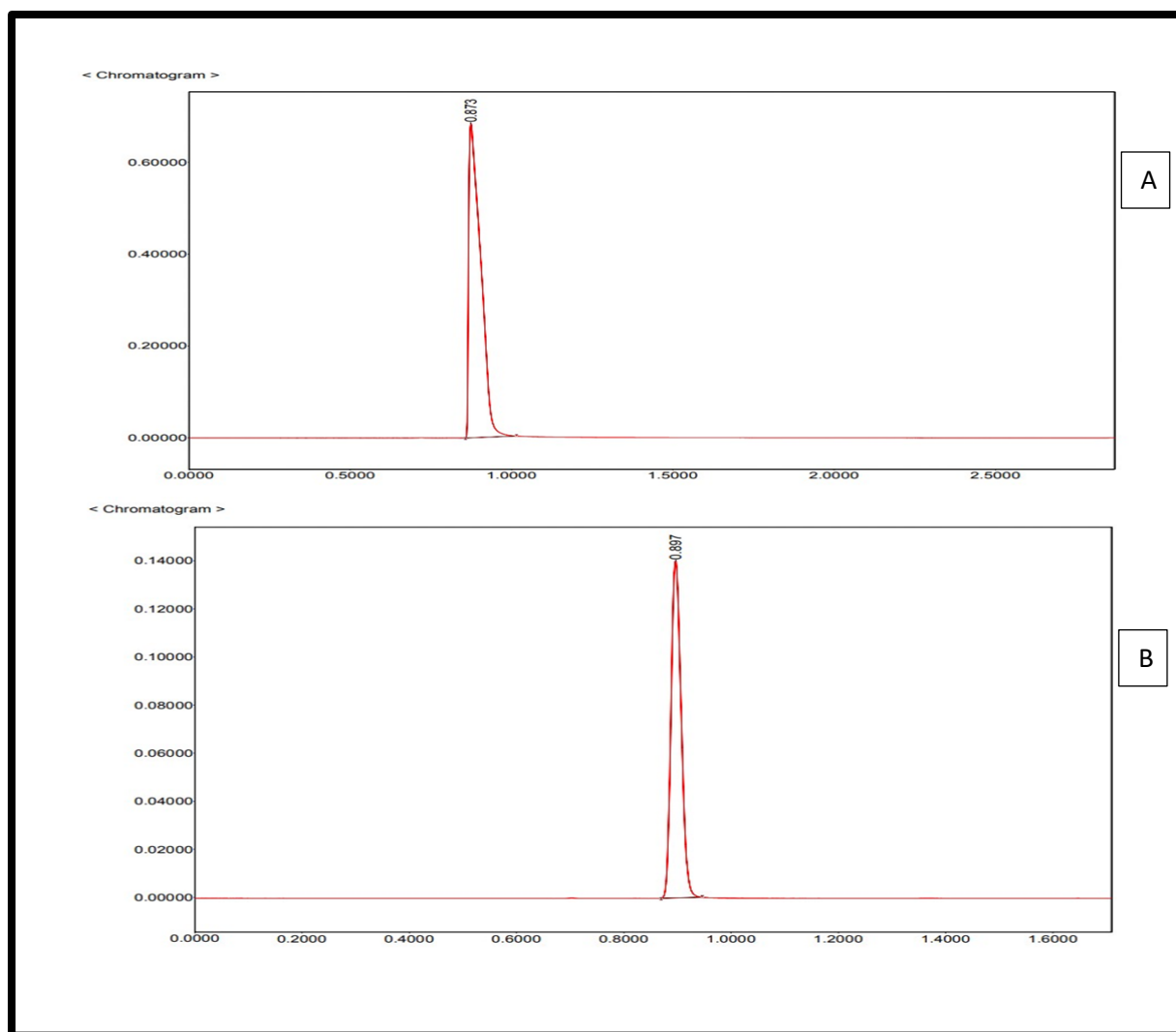


Figure 5.26 GC chromatograph (a) Standard acetonitrile (b) PLHNCs

As shown in Table 5.22 it was confirmed that acetonitrile present in final optimized batch was much below the daily limits of exposure as per ICH guidelines for residual solvents.

Table 5.22 Residual solvent analysis by GC

Sr No.	Standard Acetonitrile (ppm)	PLHNCs acetonitrile observed (ppm)	Permissible limit (ppm)
1	1000	104.2 ppm	410 ppm

PART B: FORMULATION OF EXEMESTANE LOADED PLHNCs**5.7 Formulation and Development****5.7.1 Method of preparation**

Formulations of PLHNCs was carried using modified single-step nano-precipitation method which involves self-assembly of polymers and various ratios of lipids. Two phases (organic and aqueous) were prepared separately and then mixed to form PLHNCs. A fixed quantity of PLGA 50:50 (1 – 10 mg/ml) and Exemestane were dissolved in acetonitrile to prepare the organic phase. Phospholipon 90G: DOPE: DSPE-PEG₂₀₀₀ were dissolved in 4% ethanolic solution to form aqueous phase. The resultant solution was heated at 65°C to ensure the phase transition of the lipid-bi-layer, when mixed further. After that, Exemestane containing PLGA solution was added to the preheated lipid solution via dropwise method at 1mL/min flow rate under vigorous mixing at 300 to 1500 rpm for at least 0.5 to 3.0 h to ensure a complete evaporation of the organic solvent and maximum encapsulation of Exemestane in PLHNCs. Furthermore, PLHNCs suspension was passed through laboratory manual extruder to improve the particle size distribution and polydispersity index.

5.7.2 Preliminary screening study for formulation and process parameters

Polymer selection, amount of polymer, polymer to lipid ratio, lipid composition and drug input were identified as formulation factors, while stirring time, stirring speed and no. of extrusions were identified as process parameters that may alter quality profile of product. The target profile of the intended Exemestane PLHNCs was : (1) high drug encapsulation efficiency (2) particle size below 200 nm and (3) storage stability.

5.7.3 Selection of polymer

Polymeric nanoparticles were formed by Single step nanoprecipitation in which different synthetic polymers (i.e., Polycaprolactone, Poly lactic acid, PEI, PLGA (50:50), PLGA (75:25), PLGA – PEG and PCL PEG were investigated.

Table 5.23 Selection of polymer

Polymer (10 mg/ml)	Size (nm)	PDI	Encapsulation Efficiency (%)	Zeta Potential (mV)
Polycaprolactone (PCL)	358.7 ± 9.34	0.418 ± 0.17	48.4 ± 2.63	-18.5 ± 1.5

Poly lactic acid (PLA)	413.6 ± 13.68	0.356 ± 0.21	53.2 ± 1.86	-16.4 ± 2.3
Poly glycolic acid (PGA)	363.4 ± 7.65	0.384 ± 0.19	45.1 ± 2.29	-17.1 ± 1.4
Poly D,L-lactic-co-glycolic acid (PLGA) (75:25)	256.5 ± 3.17	0.218 ± 0.08	53.2 ± 3.17	-8.5 ± 1.1
Poly D,L-lactic-co-glycolic acid (PLGA) (50:50)	126.4 ± 5.64	0.316 ± 0.14	76.8 ± 2.24	-15.6 ± 2.1
Polyethyleneimine (PEI)	276.6 ± 6.84	0.328 ± 0.26	47.4 ± 1.67	-11.7 ± 0.8
Chitosan	329.2 ± 3.85	0.527 ± 0.28	56.2 ± 2.13	13.7 ± 1.3
PLGA:PEG	186.5 ± 2.16	0.256 ± 0.18	65.34 ± 2.36	-7.5 ± 1.2
PCL:PEG	264.8 ± 5.21	0.315 ± 0.24	59.64 ± 2.15	-11.6 ± 1.4

From various polymers, PLGA (50:50) was selected for the preparation of PLHNCs based on encapsulation efficiency, size, and zeta potential (Table 5.25).

5.8.4 Effect of polymer concentration on encapsulation efficiency and particle size:

As presented in Table 5.24, increasing the concentration of PLGA resulted in increased encapsulation efficiency of exemestane up to 5 mg/ml. As polymer concentration increased, the internal core volume for drug encapsulation also increased leading to a higher encapsulation efficiency. With increasing concentration of polymer, gradual decrease in particle size was noted. After 5 mg/mL polymer concentration, EE decreased and particle size was found to increase. As the polymer concentration increased, zeta potential of the PLHNCs shifted from positive to negative charge due to negative charge of the PLGA.

Table 5.24 Effect of polymer concentration on exemestane encapsulation

Sr No.	Polymer concentration (mg/mL)	Encapsulation Efficiency (%)	Size (nm)	Zeta Potential (mV)
1	1	24.61 ± 1.24	328.4 ± 14.16	13.6 ± 1.38
2	2	42.18 ± 2.31	256.3 ± 12.41	6.5 ± 0.59
3	3	53.34 ± 1.65	205.3 ± 9.53	-3.6 ± 0.28
4	4	65.52 ± 2.26	171.2 ± 5.18	-10.2 ± 0.74
5	5	86.47 ± 3.54	135.6 ± 4.36	-18.7 ± 1.25
6	6	68.63 ± 2.63	221.8 ± 9.38	-26.5 ± 2.81

5.7.5 Effect of lipid to polymer ratio on drug encapsulation and particle size

From Table 5.25, the percentage weight ratio of lipid/polymer which could achieve exemestane encapsulation above 80% was between 20 to 30%. Above 30% weight ratio, PDI was much wider, particle size was more than 200 nm, and formulation showed two peaks as seen in Figure 5.27 as the excess and unreacted lipids may have formed liposomes separately. The nanoparticles with 35% lipids showed zeta potential of +30.6 mV suggesting the formation of liposomes (due to excessive lipids) which contributes to the high cationic charge in formulations. The zeta potential of PLHNCs with lower L/P ratio shows negative zeta potential which indicates formation of polymeric nanoparticles rather than PLHNCs. Due to these reasons, for further study, we optimized 20 % L/P ratio

Table 5.25 Effect of L/P ratio on Exemestane encapsulation

Sr. No.	L/P Percentage ratio (%)	Mole Fraction (DOPE: P90G: DSPE-PEG ₂₀₀₀)	Entrapment (%)	Size (nm)	Zeta Potential (mV)	PDI
1	5	30:40:30	48.6 ± 2.3	86.7 ± 3.4	-15.6 ± 1.9	0.185 ± 0.021
2	10	30:40:30	57.8 ± 3.2	98.6 ± 4.8	-8.7 ± 0.9	0.211 ± 0.029
3	15	30:40:30	68.4 ± 3.4	108.7 ± 5.1	1.5 ± 0.6	0.263 ± 0.041
4	20	30:40:30	86.2 ± 4.1	133.4 ± 3.6	8.3 ± 1.2	0.071 ± 0.018
5	25	30:40:30	89.6 ± 4.3	185.6 ± 6.2	17.8 ± 2.1	0.184 ± 0.027
6	30	30:40:30	90.4 ± 3.2	212.9 ± 4.2	25.4 ± 2.8	0.359 ± 0.042
7	35	30:40:30	91.1 ± 4.6	254.1 ± 5.9	30.6 ± 3.5	0.512 ± 0.052

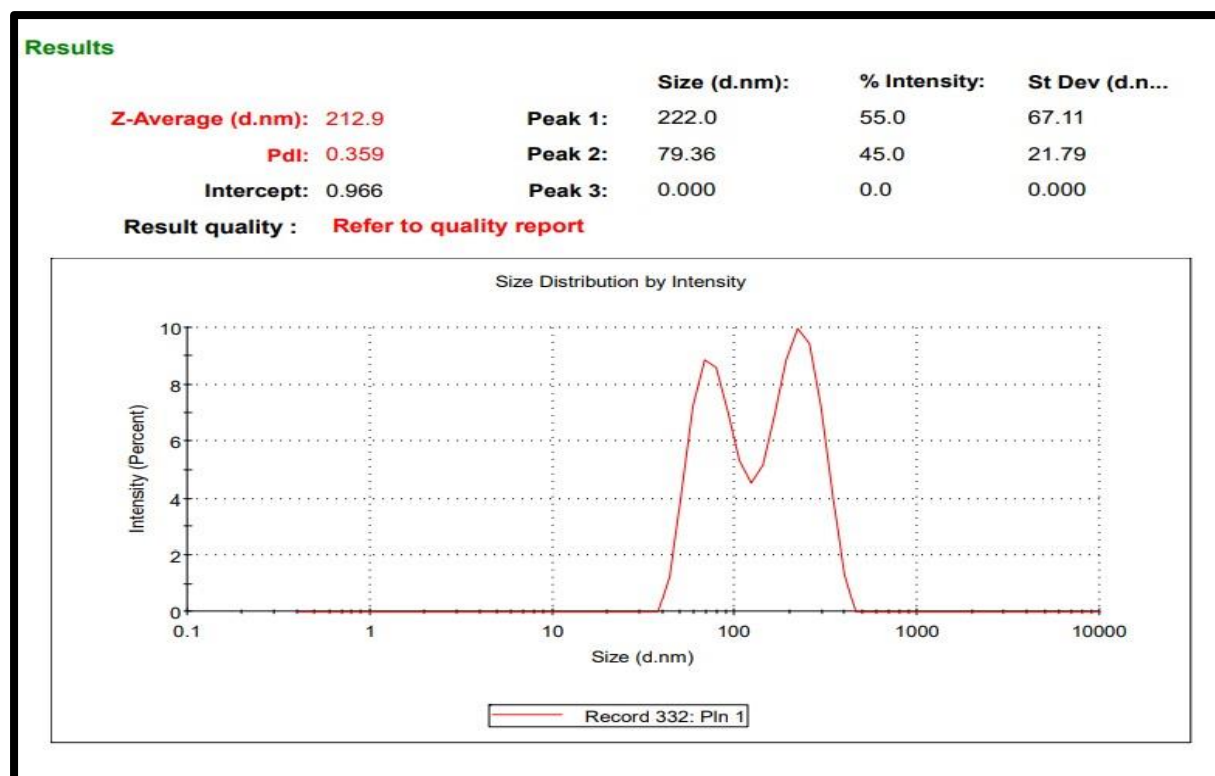


Figure 5.27 Particle Size distribution of batch with L/P ratio 35%

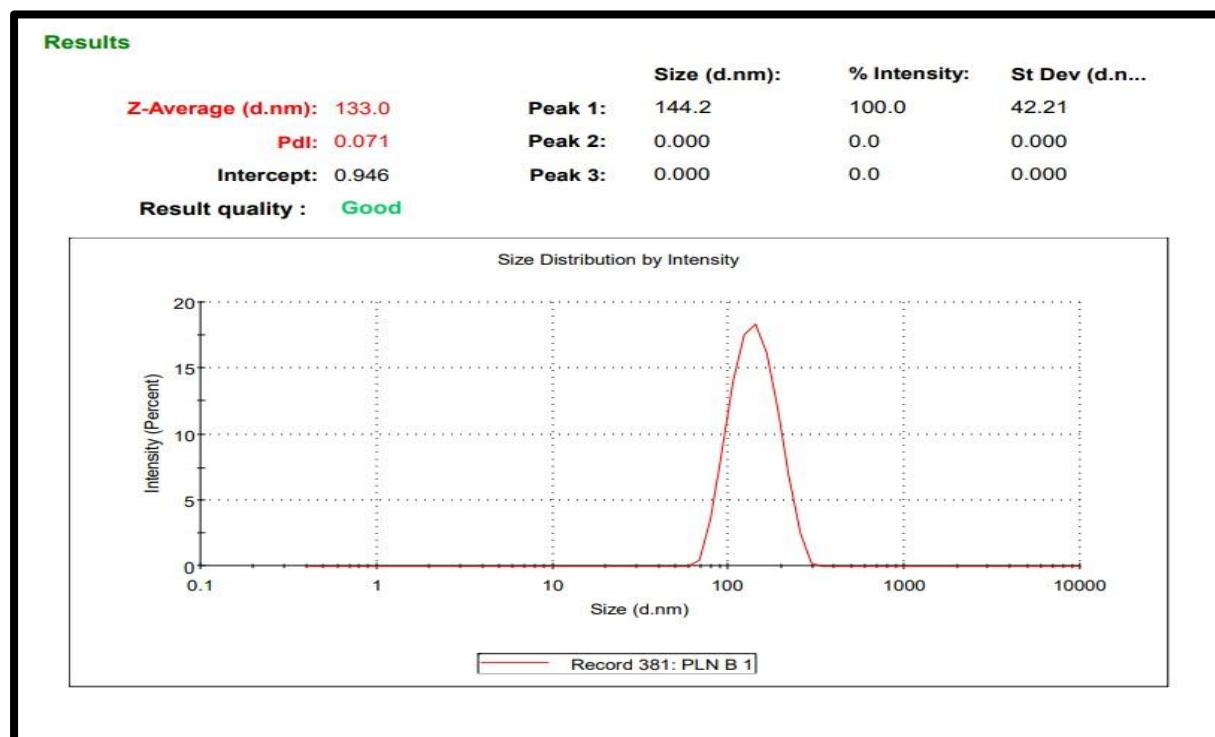


Figure 5.28 Particle Size distribution of batch with L/P ratio 20%

5.7.6 Effect of drug input on encapsulation efficiency and particle size

As displayed in Table 5.26, as the initial drug input was increased from 5 % to 15%, size reduced and drug encapsulation increased gradually. However, as the drug input further

increased to 20% and 25%, there was reduction in encapsulation efficiency and increase in particle size, since the polymer as well as lipid was insufficient to encapsulate the drug.

Table 5.26 Effect of drug input on Exemestane encapsulation

Sr. No.	Drug input (%w/w of polymer)	Entrapment Efficiency (%)	Size (nm)	Zeta Potential (mV)
1	5	74.8 ± 3.6	184.52 ± 3.4	16.5 ± 1.5
2	10	82.1 ± 2.5	153.61 ± 2.5	27.1 ± 2.2
3	15	88.5 ± 3.1	129.24 ± 5.8	31.6 ± 1.9
4	20	75.6 ± 2.2	206.48 ± 3.7	23.4 ± 2.1
5	25	68.7 ± 1.8	268.32 ± 4.4	26.8 ± 1.7

5.8.7 Effect of Number of Extrusions on encapsulation and particle size

After evaporation of organic phase, the formulation was subjected to repetitive extrusion using laboratory manual extruder (Avastin LF-1) to optimize the encapsulation efficiency and particle size of the PLHNCs (Table 5.27).

Table 5.27 Effect of no. of extrusions on encapsulation efficiency and particle size

Extrusion Cycles	Encapsulation efficiency (%)	Particle Size (nm)	PDI
1	79.24 ± 2.84	139.7 ± 5.3	0.416 ± 0.021
2	82.31 ± 3.18	131.8 ± 3.8	0.389 ± 0.013
3	83.43 ± 2.68	127.2 ± 4.2	0.354 ± 0.009
4	86.68 ± 3.24	118.3 ± 3.6	0.076 ± 0.008
5	80.38 ± 2.65	132.6 ± 5.4	0.265 ± 0.004
6	75.62 ± 3.84	145.5 ± 6.1	0.324 ± 0.011

For number of extrusions up to 4, there was significant improvement in EE, PDI and particle size reduced, but as number of extrusions were increased, the particle size and PDI both increased and EE decreased due to excessive attrition force as the force disrupts the lipid core and drug present at lipid polymer interface leaches out.

5.8 QUALITY BY DESIGN

5.8.1 Plackett-Burman design for screening study (Primary design):

The results of preliminary study were useful to detect formulation-related and process-related parameters and to understand the source of variables to improve the quality of product to assist formulation and process. Key product attributes recognized as particle size and encapsulation efficiency were evaluated for different variables. The goals of applying design were to achieve the highest encapsulation of exemestane along with the narrow particle size distribution.

Table 5.28 Variables and levels selected for preliminary study

Factor	Name	Unit	Low actual	High actual
A	Polymer concentration	mg/mL	1	6
B	Lipid/Polymer ratio	%	5	35
C	Drug input	%	10	30
D	Stirring speed	rpm	300	1200
E	Stirring time	H	0.5	4
F	Sonication time	s	20	100
G	Number of Extrusions	-	1	6

The Plackett-Burman study design has been implemented for screening of various formulation and process-related parameters i.e., polymer concentration (mg/mL) (Factor A), lipid/polymer percentage (%) (Factor B), Drug input (%) (Factor C), stirring speed (RPM) (Factor D), stirring time (h) (Factor E), sonication time (S) (Factor F), Number of extrusions (Factor G) and its impact on encapsulation efficiency and particle size distribution. For the screening study, 7 factors were evaluated at the lowest level (-1) and highest level (+1) which is shown in Table 5.29.

Table 5.29 Design Matrix of Plackett Burman Design

Run	Factor A Polymer Conc. (mg/mL)	Factor B L/P ratio (%)	Factor C Drug input (%)	Factor D Stirring speed (rpm)	Factor E Stirring Time (H)	Factor F Sonication Time (Sec)	Factor G Number of Extrusion	Response -1 % EE (%)	Response -2 Particle Size (nm)
-----	---	------------------------------------	----------------------------------	---	-------------------------------------	---	---------------------------------------	-------------------------------	--

1	6	5	30	1500	4	20	1	69.21	158.7
2	1	35	30	300	4	100	6	58.36	135.8
3	1	35	30	1500	0.5	20	1	52.34	123.6
4	1	35	10	1500	4	20	6	57.63	118.1
5	1	5	10	1500	0.5	100	6	46.95	131.5
6	6	5	30	1500	0.5	100	6	67.55	168.9
7	6	35	30	300	0.5	20	6	85.43	239.5
8	6	35	10	300	0.5	100	1	66.44	265.1
9	6	35	10	1500	4	100	1	71.29	275.6
10	1	5	10	300	0.5	20	1	42.78	128.4
11	6	5	10	300	4	20	6	62.43	210.2
12	1	5	30	300	4	100	1	54.31	132.8

5.8.1.1 ANOVA for encapsulation efficiency (Factorial model)

Multi-linear regression analysis and ANOVA (Table 5.30) have been performed to analyse the data, and a series of Pareto charts were constructed to demonstrate the influence of each parameter on encapsulation efficiency.

Table 5.30 ANOVA for encapsulation efficiency

Source	Sum of squares	Degree of Freedom	Mean square	F – Value	p-value (prob>F)
Model	1510.81	9	167.87	4297.44	0.0014
A: Polymer Conc.	1006.32	1	1006.32	716.87	0.0002
B-L/P	118.78	1	118.78	507.24	0.0020
C-Drug input	149.18	1	149.18	637.08	0.0016
D-Stirring Speed	21.43	1	21.43	91.51	0.0108
E-Stirring time	59.36	1	59.36	253.50	0.0039
F-Sonication Time	47.24	1	47.24	201.73	0.0049
G-Number of Extrusions	64.00	1	64.00	273.29	0.0036
AB	110.29	1	110.29	471.00	0.0021
AE	12.57	1	12.57	53.66	0.0181
Model Statistics					
Standard Deviation				0.48	

Mean	61.22
R ²	0.9997
Adequate Precision	96.692

The Model F-value of 4297.44 implies that the model is significant. There is only a 0.14% chance that a "Model F-Value" this large could occur due to noise. Values of "Prob > F" less than 0.0500 indicate model terms are significant. In this case A, B, C, D, E, F, G, AB, AE were significant model terms. The adequate precision of 96.692 indicates an adequate signal. This model can be used to navigate the design space.

Hence we can conclude that the polymer concentration (A), Lipid to polymer ratio (B), Drug input (C), Stirring speed (D), Stirring time (E), Sonication (F) and Number of Extrusions (G) are the potential factors that affect the encapsulation efficiency of the PLHNCs. Further there were significant interactions between Factor A and B which was justified by following Box-Behnken design. Other interactions between A&F, D&G and A&C were found to be less significant hence it had no impact on the encapsulation efficiency of PLHNCs.

5.8.1.2 Influence of factors on encapsulation efficiency (Pareto Chart)

As represented in Figure 5.29 as factor A (Polymer concentration) had crossed the Bonferroni limit, it possessed the utmost importance for increasing encapsulation efficiency, while factor B (L/P ratio) and C (Drug input) may have an intermediate effect on the encapsulation efficiency as these factors could cross the t-critical value limit. Further, there were significant interactions between factor A & B and A & E. Other interactions between factor D & G and the factor C & F were not found significant and it had no impact on the encapsulation efficiency of PLHNCs.

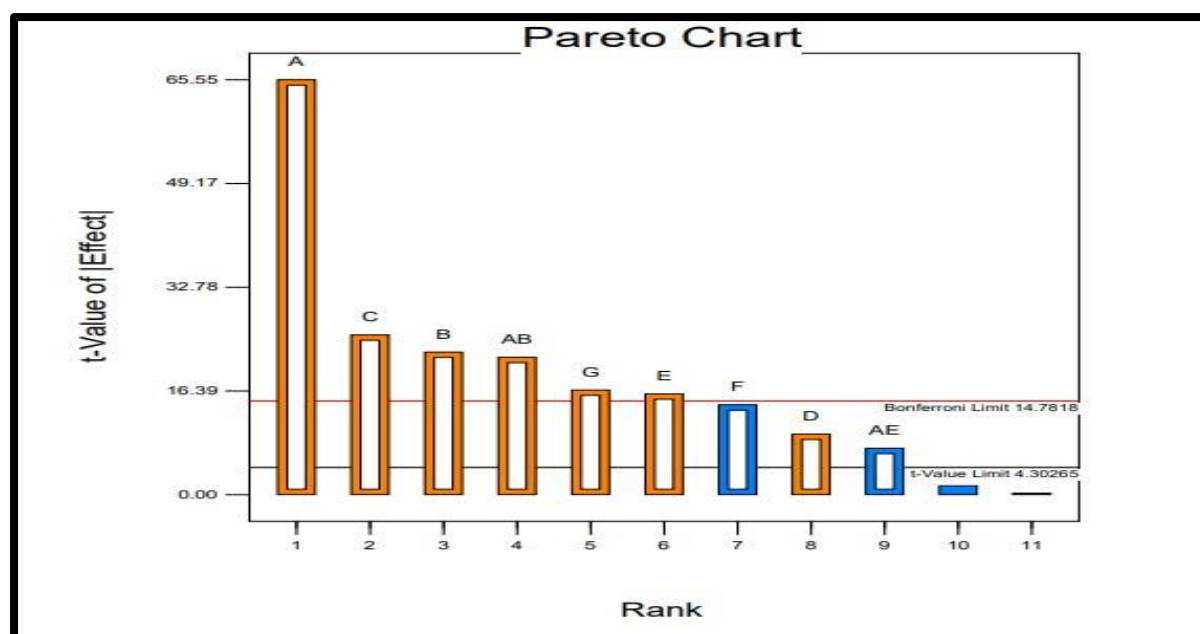


Figure 5.29 Pareto Chart for Encapsulation efficiency

The Pareto chart depicted that independent variable such as concentration of polymer, lipid to polymer percentage ratio and drug input exerted a most significant effect (Above t-value limit) on the response variables.

5.8.1.3 ANOVA for Particle Size (Factorial model)

Multi-linear regression analysis and ANOVA (Table 5.31) have been performed to analyse the data, and a series of Pareto charts were constructed to demonstrate the influence of each parameter on the particle size of PLHNCs.

Table 5.31 ANOVA for particle size

Source	Sum of squares	Degree of Freedom	Mean square	F – Value	p-value (prob>F)
Model	37086.30	7	5298.04	966.31	< 0.0001
A-Polymer Conc.	25007.07	1	25007.07	204.32	< 0.0001
B-L/P	2114.27	1	2114.27	81.70	0.0008
C- Drug input	524.16	1	524.16	20.25	0.0108
F-Sonication Time	1.74	1	1.74	0.067	0.8081
G- Number of Extrusion	177.98	1	177.98	6.88	0.0586
AB	3074.70	1	3074.70	118.81	0.0004
AC	1278.06	1	1278.06	49.39	0.0022

Model Statistics	
Standard Deviation	5.09
Mean	174.09
R ²	0.9972
Adequate Precision	35.95

The Model F-value of 966.31 implies the model is significant. There is only a 0.01% chance that a "Model F-Value" this large could occur due to noise. Values of "Prob > F" less than 0.0500 indicate model terms are significant. In this case A, B, C, AB, AC are significant model terms. Values greater than 0.1000 indicate the model terms are not significant. A ratio greater than 4 is desirable. The ratio of 35.952 indicates an adequate signal. This model can be used to navigate the design space. Hence, we can conclude that polymer concentration (A), Lipid to polymer ratio (B) and Drug input (C) are the potential factors that affect the particle size of the PLHNCs and there is potential interaction between A & B and between A & C that affects the particle size of PLHNCs which was further explored by Box Behnken design.

5.8.1.4 Influence of factors on Particle Size (Pareto Chart)

As observed in Figure 5.30, factor A (i.e., polymer concentration) and factor B (i.e., lipid to polymer ratio) crossed the Bonferroni limit, as they possessed the utmost importance for increasing the particle size. Another factor C (i.e., Drug input) may have an intermediate effect on the encapsulation efficiency as it did cross the t-critical value limit. Further, there was a significant interaction between A & B and A & C, but other significant interactions were not found between any other factors.

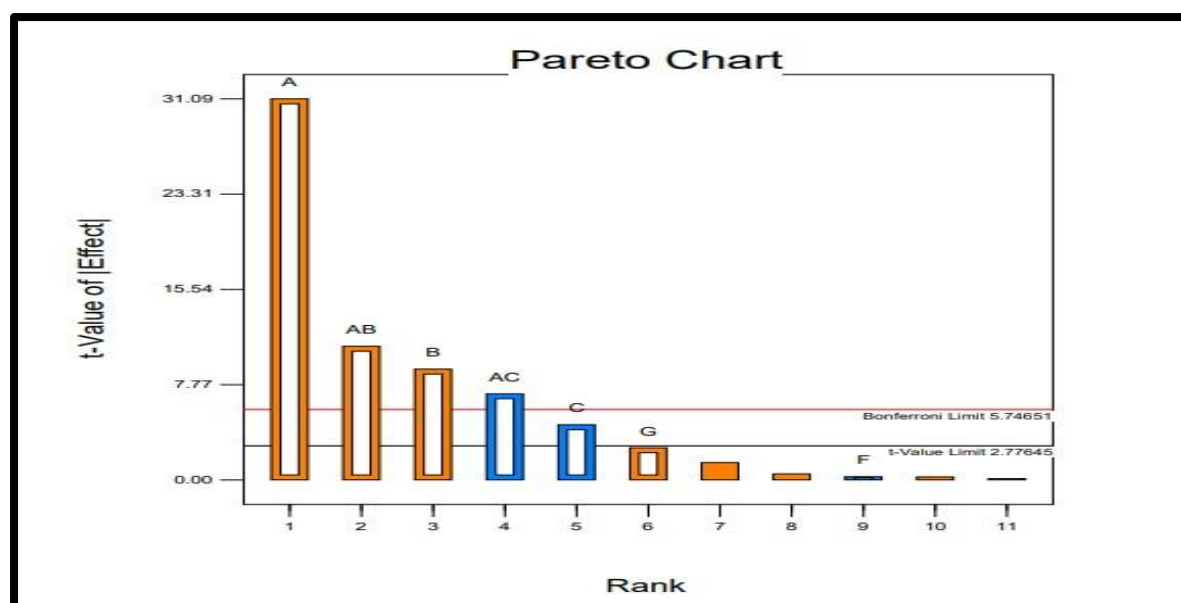


Figure 5.30 Pareto Chart for the selected factorial model of Particle Size

The Pareto chart depicts that independent variables A (i.e., polymer concentration), B (i.e., lipid to polymer percentage) and C (i.e., Drug input) have a significant impact on the particle size of the PLHNCs (above t-value limit).

5.8.2 Box Behnken design for point prediction (Secondary design)

Based on the results of the primary factor screening design, three variables (i.e., polymer concentration, lipid to polymer percentage and Drug input) were selected for further optimization (Table 5.32) using Box-Behnken design. A suitable design (Table 5.33) has been developed that integrates independent variables and generates the final equations that can result into a theoretical outcome for the response.

Table 5.32 Variables and levels selected based on primary design

Independent variables	Unit	Levels	
		-1	+1
A: Polymer concentration	mg/mL	2	6
B: Lipid to polymer ratio	%	10	30
C: Drug input	% w/w	10	30
Dependent variables	Unit		
Encapsulation Efficiency	Percentage		
Particle Size	nm		

Table 5.33 Design matrix of Box -Behnken Design

Run	Factor A Polymer Concentration (mg/mL)	Factor B L/P ratio (%)	Drug input (% w/w)	Response – 1 Encapsulation Efficiency (%)	Response – 2 Particle Size (nm)
1	2	10	20	57.84	231.2
2	4	30	30	82.41	119.5
3	2	30	20	68.19	175.3
4	4	10	10	71.63	172.6
5	4	20	20	83.64	123.5
6	4	10	30	78.24	118.6
7	2	20	30	62.18	253.6
8	2	20	10	56.46	239.2
9	4	20	20	84.04	123.1
10	6	10	20	65.32	198.5
11	4	20	20	83.19	125.9
12	6	20	10	59.84	294.6
13	6	20	30	64.51	209.8
14	4	30	10	78.54	133.5
15	6	30	20	65.25	224.8

5.10.2.1 Statistical analysis of response: Encapsulation efficiency

5.10.2.1.1 ANOVA results of different models

Multi-linear regression analysis and ANOVA (Table 5.34) have been performed to analyse the data, and a series of response surface plots were constructed to demonstrate the influence of each parameter on encapsulation efficiency of PLHNCs.

Table 5.34 Summary of ANOVA for Encapsulation efficiency

Source	Sequential	Lack of fit	Adjusted R-Squared	Predicted R-Squared	Suggested model
	p-value	p-value			
Linear	0.7881	0.0013	-0.1610	-0.6055	

2FI	0.9802	0.0009	-0.5603	-2.2845	
Quadratic	<0.0001	0.7367	0.9988	0.9966	Suggested
Cubic	0.0015	0.5744	0.9982		Aliased

Highest polynomial showing the lowest p value (<0.05) along with highest Lack of Fit p-value (>0.1) was considered for model selection. Based on the criteria, quadratic model was found to be best fitted to the observed responses. (Table 5.34).

Table 5.35 ANOVA results for encapsulation efficiency

Source	Sum of Squares	df	Mean Square	F – Value	p-value Prob > F	
Model	1419.00	9	157.67	1284.37	< 0.0001	Significant
A – Polymer concentration	13.13	1	13.13	106.98	0.0001	
B – Lipid to polymer ratio	57.03	1	57.03	464.58	< 0.0001	
C – Drug input	54.44	1	54.44	443.51	< 0.0001	
AB	27.14	1	27.14	221.12	< 0.0001	
AC	0.28	1	0.28	2.25	0.1943	
BC	1.88	1	1.88	15.29	0.0113	
A²	1225.11	1	1225.11	9979.88	< 0.0001	
B²	5.84	1	5.84	47.59	0.0010	
C²	80.20	1	80.20	653.28	< 0.0001	
Residual	0.61	5	0.12			
Lack of fit	0.25	3	0.084	0.46	0.7367	Not significant
Pure Error	0.36	2	0.18			
Cor Total	1419.62	14				
ANOVA Summary						
Parameters	Results		Parameters		Results	
Std. Dev.	0.35		R – Squared		0.9996	
Mean	70.75		Adj. R – Squared		0.9988	

C.V %	0.50	Pred R – Squared	0.9966
Press	4.85	Adeq. Precision	94.480

The ANOVA table revealed that the effect of factors was significant and hence the model is significant for the Encapsulation Efficiency. The F-value was highest for the factor B (464.58), i.e., increasing the lipid to polymer ratio would increase the entrapment of exemestane in quadratic manner. Factor C (drug input having F-value 443.51) had almost same significance as that of the factor B, but factor A, polymer concentration had low effect on encapsulation of drug which can be observed from the surface plots.

The Model F-value of 1284.37 implies the model is significant. There is only a 0.01% chance that a "Model F-Value" this large could occur due to noise. Values of "Prob > F" less than 0.0500 indicate model terms are significant. In this case A, B, C, AB, BC, A², B², C² are significant model terms. Values greater than 0.1000 indicate the model terms are not significant. The "Lack of Fit F-value" of 0.46 implies the Lack of Fit is not significant relative to the pure error. There is a 73.67% chance that a "Lack of Fit F-value" this large could occur due to noise. The "Pred R-Squared" of 0.9966 is in reasonable agreement with the "Adj R-Squared" of 0.9988. The adequate precision of 94.480 indicates an adequate signal.

5.8.2.1.2 Model diagnostic plots for encapsulation efficiency

5.8.2.1.2.1 Normal residual plot

In this case, as the plot looks to fit in fat pencil form (Figure 5.31), it was considered as normal

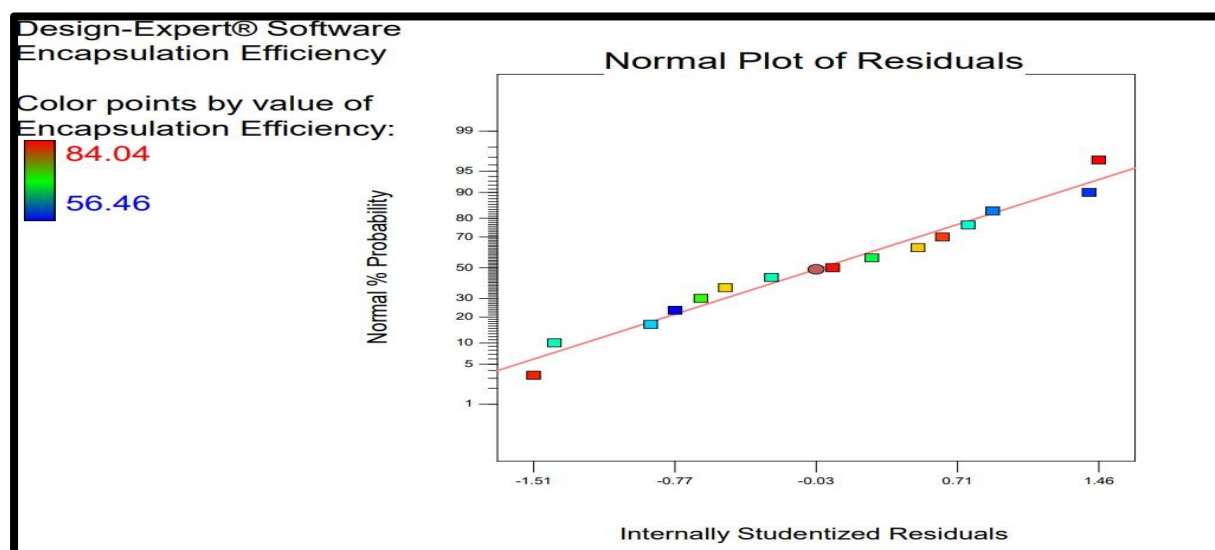


Figure 5.31 Normal plot of residuals for encapsulation efficiency

5.8.2.1.2.2 Box-Cox plot for power transformation

Plot in Figure 5.32 shows the λ value of 1, which lies near the best λ value and within 95% confidence interval of the design.

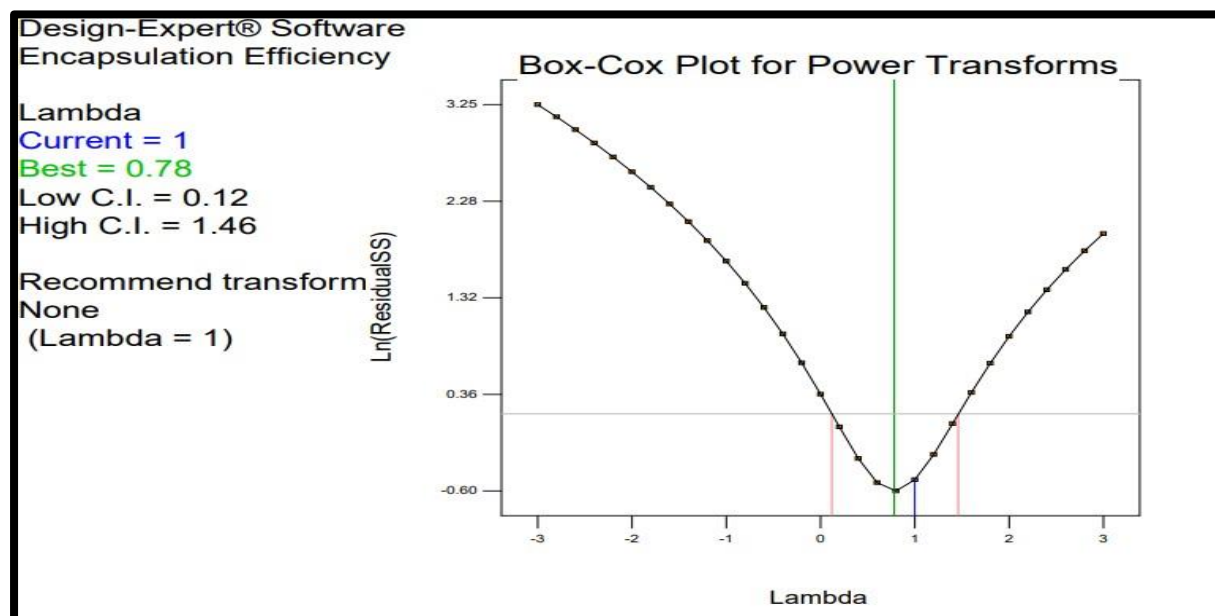


Figure 5.32 Box-Cox plot for power transformation for the encapsulation efficiency

5.8.2.1.2.3 Piepel's plot

A steep slope for factor A (Concentration of polymer) and curvature for factor B and C (Lipid to polymer percentage ratio and Drug input respectively) as shown in Figure 5.33 proves that the response was sensitive to factor. The line for the polymer concentration shows deviation which suggests that concentration of polymer has a great impact on the encapsulation efficiency.

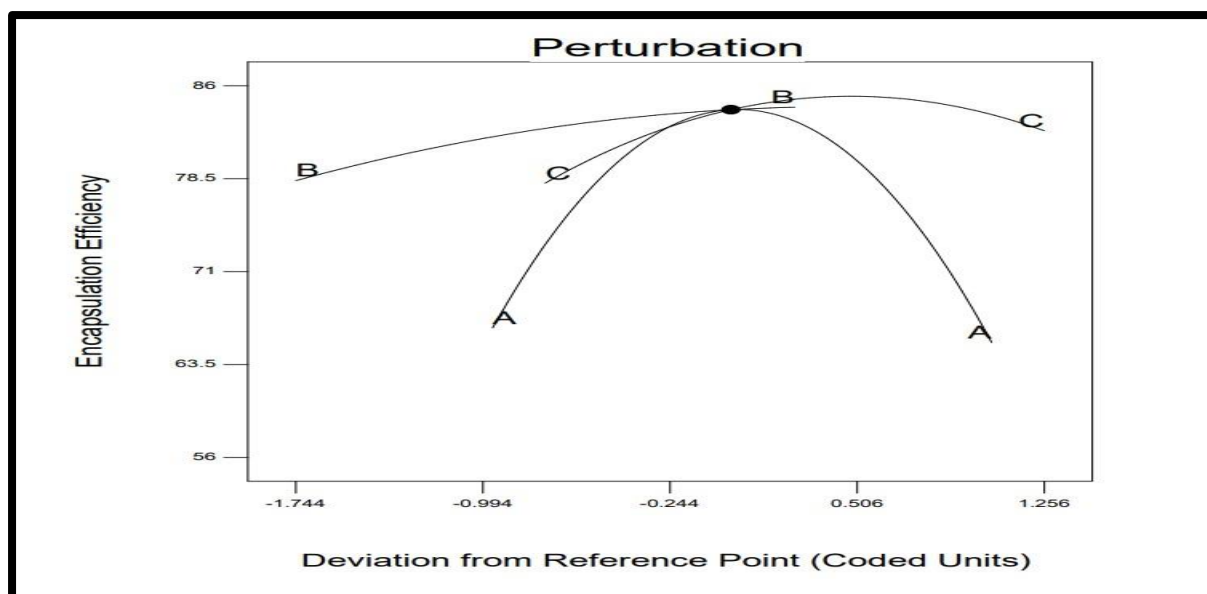


Figure 5.33 Piepel's plot

5.8.2.1.2.4 Response surface (3D) plots

The value of ANOVA gives us idea about the factors having significant effect on Encapsulation Efficiency which is shown in contour and 3D plots. The RED area in the Figure 5.34 shows the area of maximum Encapsulation Efficiency and BLUE zone represents the area with lowest Encapsulation Efficiency.

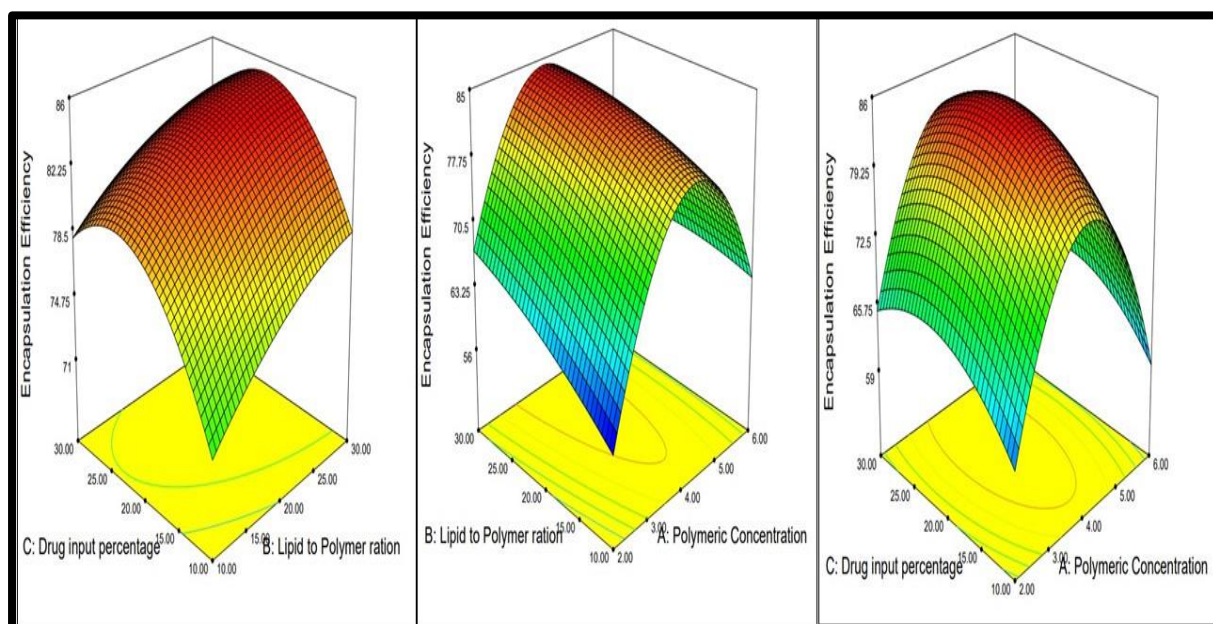


Figure 5.34 Effects of various factors on EXE entrapment by 3D surface curve

Two-factor 3D response surface plots for exemestane entrapment justifies the effect of aforementioned significant terms. A quadratic model was found to have the best fit with the

applied design. From the plots, it is concluded that increasing the concentration of exemestane and polymer initially increases the EXE entrapment but after saturation concentration the encapsulation efficiency goes down. This may be due to achievement of supersaturation by EXE solution and increased viscosity of vehicle due to increased polymer concentration, that leads to formation of larger particles that reduces overall encapsulation. All response surface (3D) show combined effect of concentration of polymer, lipid to polymer percentage and Drug input on % encapsulation efficiency. From the graph, increase in the Encapsulation Efficiency were noticed with increasing concentration of polymer and lipid to polymer ratio. The lipid to polymer ratio plays important role as lipid in addition to coating on the surface of polymer also acts as surfactant.

5.8.2.1.3 Mathematical equation for Encapsulation Efficiency

Final equation in terms of coded factors has been obtained as below:

$$\text{Encapsulation efficiency} = +83.62 + 1.28*A + 2.67*B + 2.61*C - 2.60*A*B - 0.26*A*C - 0.69*B*C - 18.22*A^2 - 1.26*B^2 - 4.66*C^2 \text{ ----- (5.4)}$$

5.8.2.2 Statistical analysis of response (dependent) variable 2: Particle size

5.8.2.2.1 ANOVA results of different models

Multi-linear regression analysis and ANOVA (Table 5.36) have been performed to analyse the data, and a series of response surface plots were constructed to demonstrate the influence of each parameter on particle size of PLHNCs.

Table 5.36 Summary of ANOVA results of different models for particle size

Source	Sequential	Lack of fit	Adjusted	Predicted	Suggested Model
	p-value	p-value	R-Squared	R-Squared	
Linear	0.8546	0.0005	-0.1893	-0.7813	
2FI	0.9414	0.0004	-0.4652	-2.5343	
Quadratic	<0.0001	0.3580	0.9989	0.9952	Suggested
Cubic	0.0006	0.3586	0.9993	NA	Aliased

Highest polynomial showing the lowest p value (<0.05) along with highest Lack of Fit p-value (>0.1) was considered for model selection. Based on the criteria, quadratic model was found to be best fitted to the observed responses.

Table 5.37 ANOVA results of quadratic model for particle size

Source	Sum of Squares	df	Mean Square	F – Value	p-value Prob > F	
Model	46794.27	9	5199.36	1449.77	< 0.0001	Significant
A – Polymer concentration	100.82	1	100.82	28.11	0.0032	
B – Lipid to polymer ratio	574.61	1	574.61	160.22	< 0.0001	
C – Drug input Percentage	2394.32	1	2394.32	667.62	< 0.0001	
AB	1689.21	1	1689.21	471.01	< 0.0001	
AC	2460.16	1	2460.16	685.98	< 0.0001	
BC	400.00	1	400.00	111.53	0.0001	
A²	35654.17	1	35654.17	9941.68	< 0.0001	
B²	828.92	1	828.92	231.13	< 0.0001	
C²	2665.17	1	2665.17	743.15	< 0.0001	
Residual	17.93	5	3.59			
Lack of fit	13.35	3	4.45	1.94	0.3580	Not significant
Pure Error	4.59	2	2.29			
Cor Total	46812.20	14				
ANOVA Summary						
Parameters	Results	Parameters	Results			
Std. Dev.	1.89	R – Squared	0.9996			
Mean	182.91	Adj. R – Squared	0.9989			
C.V %	1.04	Pred R – Squared	0.9952			
Press	223.84	Adeq. Precision	114.939			

The ANOVA table revealed that the effect of factors was significant and hence the model is significant for the particle size. The F value was the highest for the factor C (667.62), i.e., increasing the Drug input, would increase the particle size in quadratic manner. Lipid to polymer ratio and Drug input have most prominent effect as their p-value is <0.0001.

Increasing the lipid to polymer ratio leads to increased particle size. On increasing the drug input, due to increase in the overall viscosity of the system and supersaturation of drug suspension that leads to faster nucleation rate by promoting condensation and/or coagulation which results in increased particle size.

The Model F-value of 1449.77 implies the model is significant. There is only a 0.01% chance that a "Model F-Value" this large could occur due to noise. Values of "Prob > F" less than 0.0500 indicate model terms are significant. In this case A, B, C, AB, AC, BC, A², B², C² are significant model terms. Values greater than 0.1000 indicate the model terms are not significant. The "Lack of Fit F-value" of 1.94 implies the Lack of Fit is not significant relative to the pure error. There is a 35.80% chance that a "Lack of Fit F-value" this large could occur due to noise. The "Pred R-Squared" of 0.9952 is in reasonable agreement with the "Adj R-Squared" of 0.9989. The adequate precision of 114.939 indicates an adequate signal. This model can be used to navigate the design space.

5.8.2.2.2 Model diagnostic plots for Particle Size

5.8.2.2.2.1 Normal residual plots

In this case as the plot looks to fit in fat pencil (Figure 5.35), it was considered as normal.

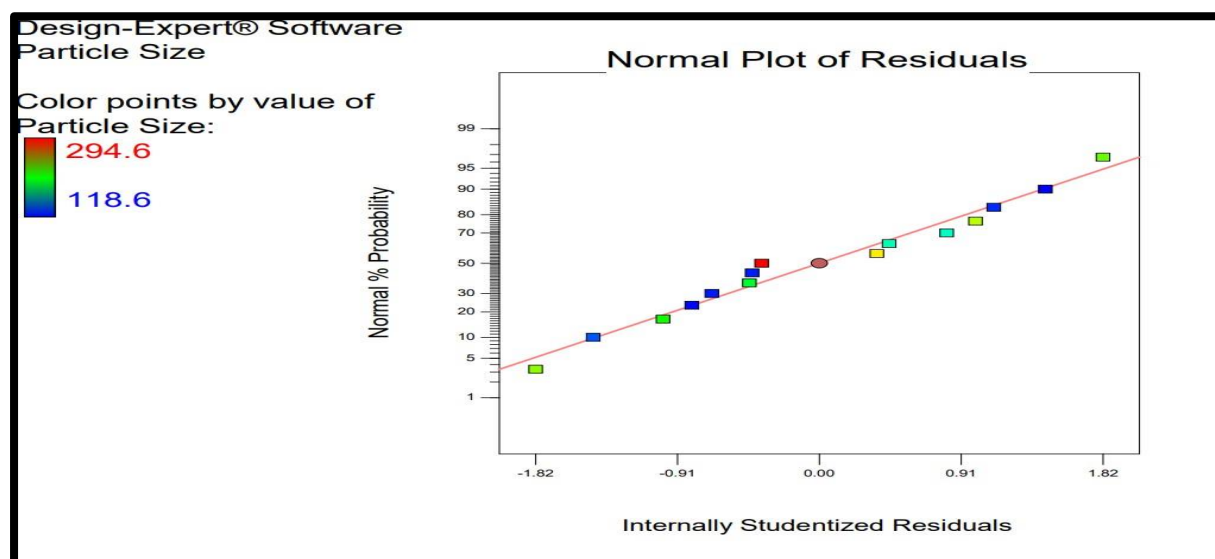


Figure 5.35 Normal plot of residuals for particle size

5.8.2.2.2.2 Box cox plot for power transformation

Figure 5.36 shows the λ value of 1, which lies near the best λ value and within 95% confidence interval of it, indicating no requirement for any power transformation.

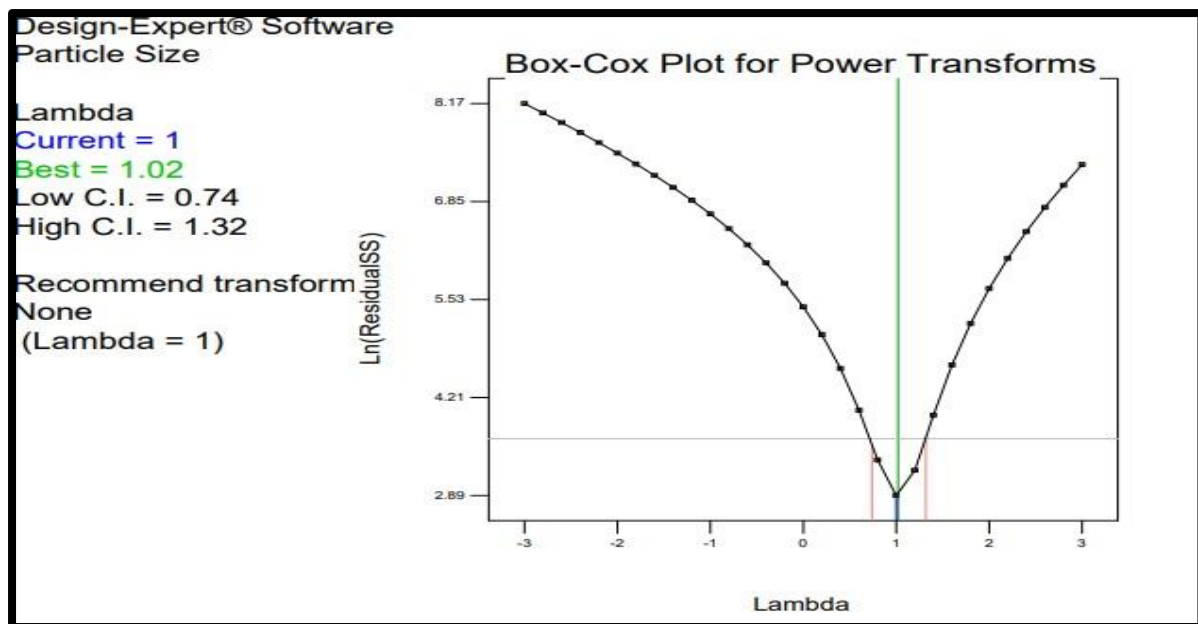


Figure 5.36 Box cox plot for power transformation for the particle size

5.8.2.2.3 Piepel's plot

A steep slope for factor A (Concentration of polymer) and curvature for factor B and C (Lipid to polymer percentage ratio and Drug input respectively) Figure 5.37 proves that the response is sensitive to factor. The line for the polymer concentration and drug input both shows deviation suggesting that they have a great impact on particle size.

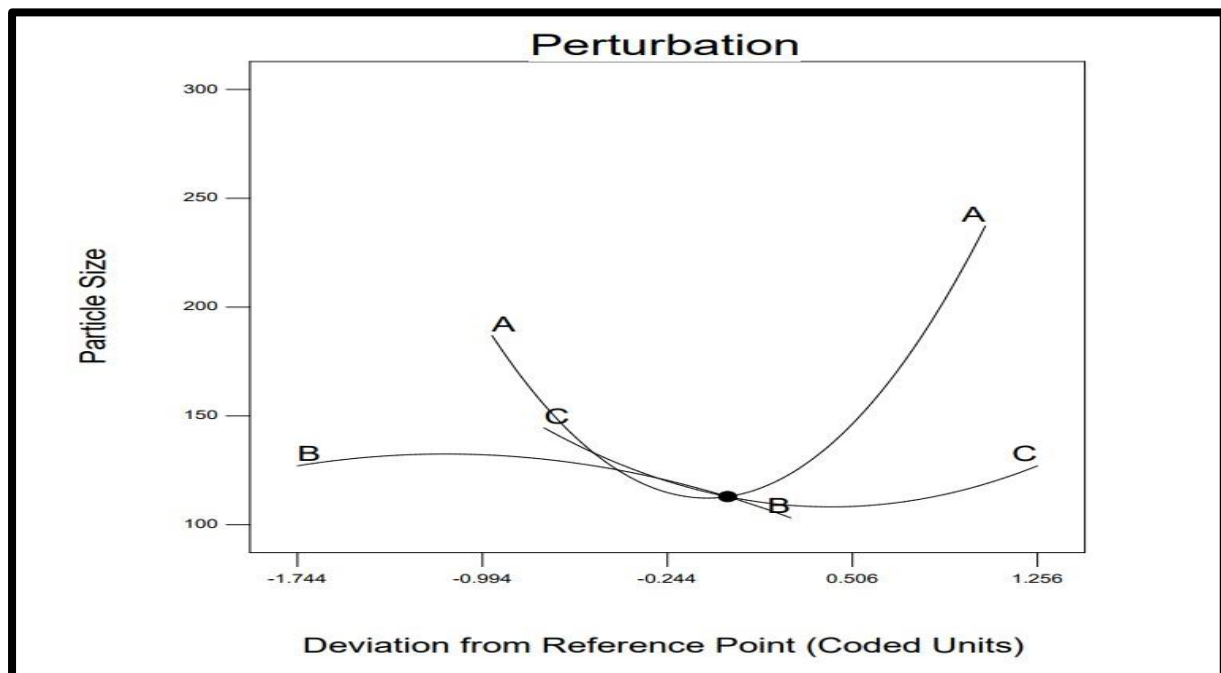


Figure 5.37 Piepel's Plot for particle size

5.8.2.2.4 Response surface (3D) plots

The value of ANOVA gives us idea about the factors having significant effect on Encapsulation Efficiency which is shown in contour and 3D plots. The RED area in the Figure 5.38 shows the area of maximum Encapsulation Efficiency and BLUE zone represents the area with lowest particle size.

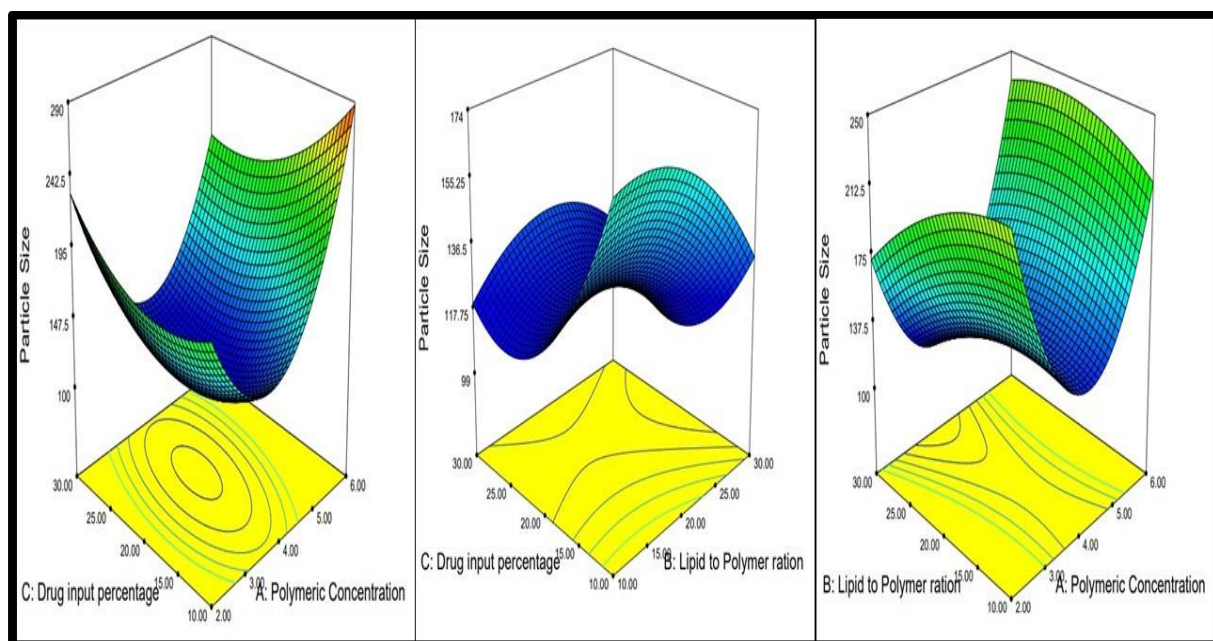


Figure 5.38 Effects of various factors on PLHNCs particle size by 3D Surface plots

Two-factor 3D response surface plots for particle size of PLHNCs justifies that the significant terms. All the response surface (3D) which shows combined effect of concentration of polymer, lipid to polymer percentage and Drug input on particle size of PLHNCs. The Response surface plots shows combined effect of polymer concentration and lipid to polymer weight ratio on PLHNCs size. As per the ANOVA data, all the three independent variables have significant effect on the particle size based on its p-value, i.e., $p < 0.05$. However, it was observed that Lipid to Polymer ratio alone does not affect the particle size based on Piepel's plot. From the plots it can be concluded that on increasing the polymer concentration and drug input, the entrapment increases and particle size decreases. But further increase in polymer concentration and drug input percentage, the particle size tends to increase. This may be due to increase in the overall viscosity of the system in presence of excess polymer and supersaturation of drug suspension that leads to faster nucleation rate by promoting condensation and/or coagulation which results in increased particle size (30).

5.8.2.2.3 Mathematical equation for particle size

$$\text{Particle Size} = +124.17 + 3.55*A - 8.47*B - 17.30*C + 20.55*A*B - 24.80*A*B + 10.00*B*C + 98.27*A^2 - 14.98*B^2 + 26.87*C^2 \text{ ----- (5.5)}$$

5.8.3 Desirability plot and overlay plot for optimization

Desirability plot was generated using Design Expert 7.0. Parameters for the desirability batch are shown in Table 5.38.

Table 5.38 Variables for desirability plot and goals for response

Name	Goal	Lower Limit	Upper Limit
A: Polymer Concentration (mg/mL)	In range	2	6
B: Lipid to Polymer percentage	In range	10	30
C: Drug input percentage	In range	10	30
Quality Target			
Encapsulation Efficiency (%)	Maximize	65	86
Particle Size (nm)	Minimize	110	165

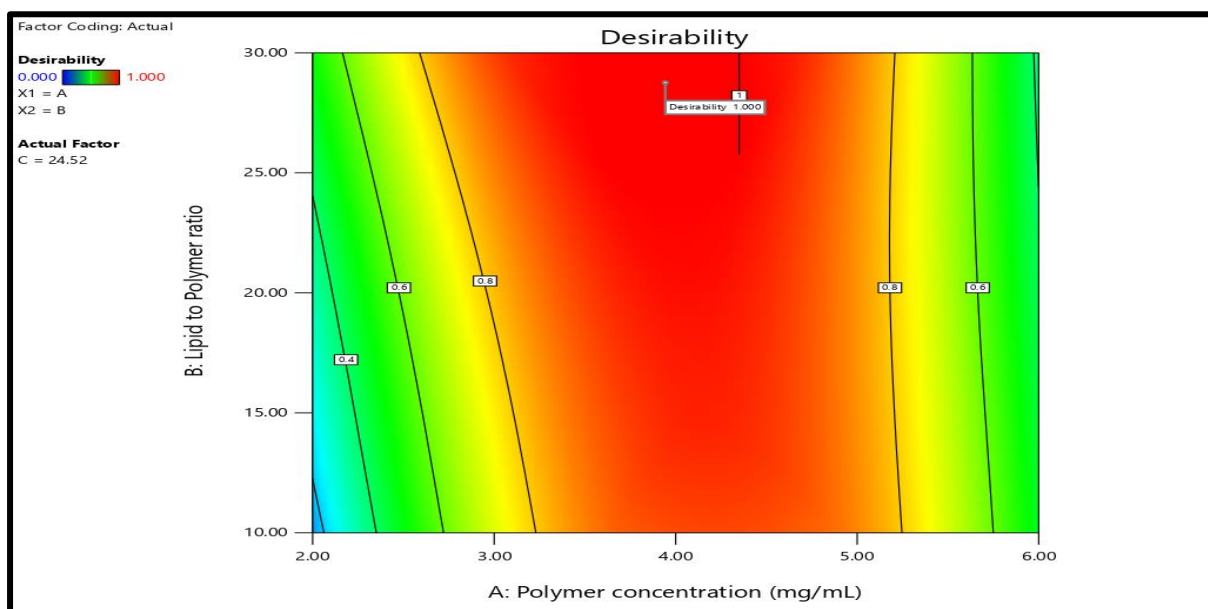


Figure 5.39 Desirability Plot

5.8.4 Point prediction and confirmation

From the Box-Behnken design, three most desirable batches were selected for further optimization and lyophilization. Confirmation of the responses was done by carrying out the experiment using selected factor values in triplicate (Table 5.39).

Table 5.39 Process parameters for optimized batch

Variables	Predicted Values	Actual values
A: Polymer Concentration (mg/mL)	3.86	4.00
B: Lipid to Polymer ratio	25.00	25.00
Drug input (%)	18.97	19.00

Table 5.40 Predicted vs Actual Experimental results

Batch No.	Parameters	Predicted values	Observed Values	%Error
1.	Encapsulation Efficiency (%)	84.85	86.84 ± 3.57	2.34
2.	Particle Size (nm)	117.9	120.8 ± 2.38	2.29

5.9 RESULTS AND DISCUSSION

5.9.1 Particle size distribution by dynamic light scattering (DLS)

The nanocarrier size obtained in the present study (Figure 5.40) was 120.8 ± 2.38 nm, with a very fine polydispersity index of 0.060 ± 0.008 .

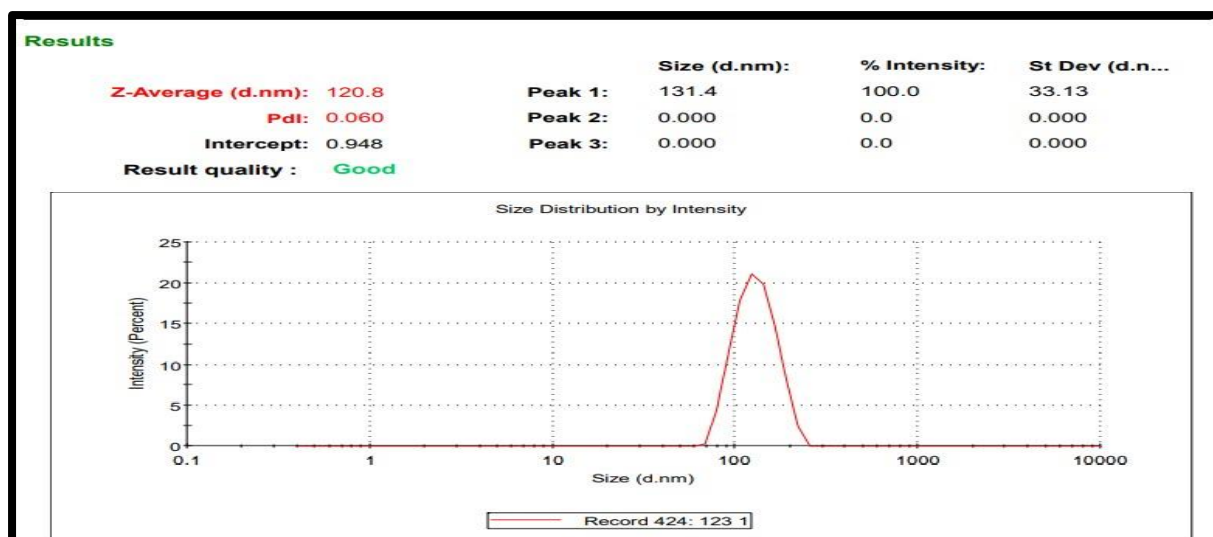


Figure 5.40 Particle size and PDI of optimized PLHNCs batch

5.9.2 Zeta Potential of optimized PLHNCs

The zeta potential of PLHNCs was found to be $+6.89 \text{ mV} \pm 0.86$ as shown in Figure 5.41. Positive zeta potential of PLHNCs was due to presence of DOPE, though it was near to the zero as the charge of nanocarrier was balanced due to presence of both cationic and anionic lipids. Positively charged PLHNCs particle will repel each other and account for stability by preventing aggregation. Moreover, Cationic charge of PLHNCs is advisable for the higher cellular uptake.

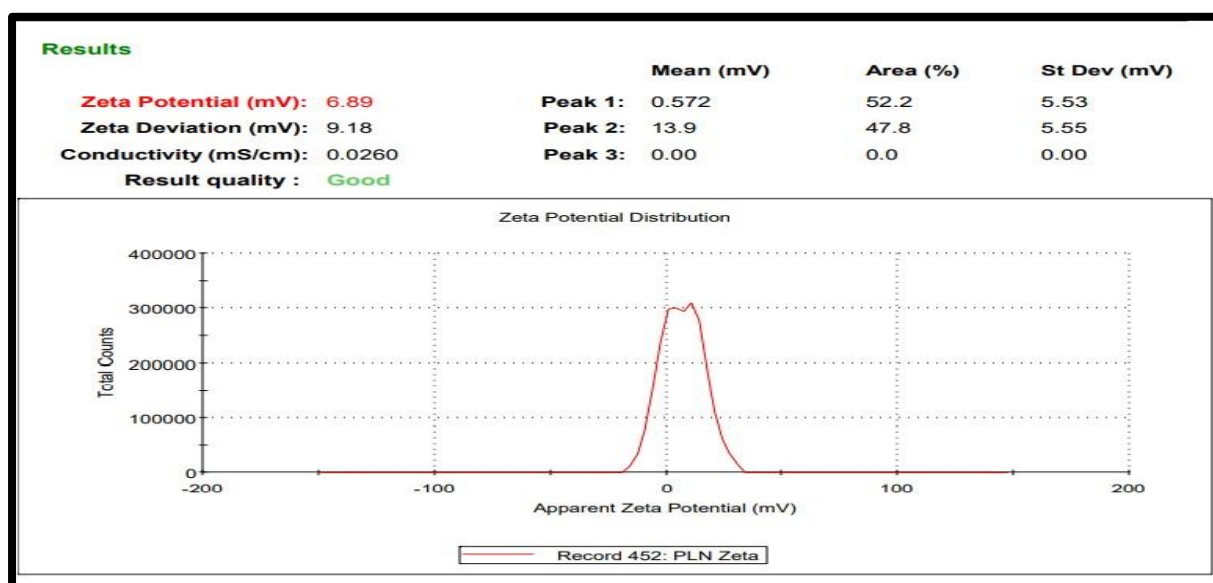


Figure 5.41 Zeta potential of optimized PLHNCs

5.9.3 Transmission Electron Microscopy (TEM)

The particle size was found to be 131.8 nm and ring diameter was less than 20 nm which confirms the morphology and architecture of PLHNCs. The negative stain separates the positively charged lipid from the polymer layer (Figure 5.42).

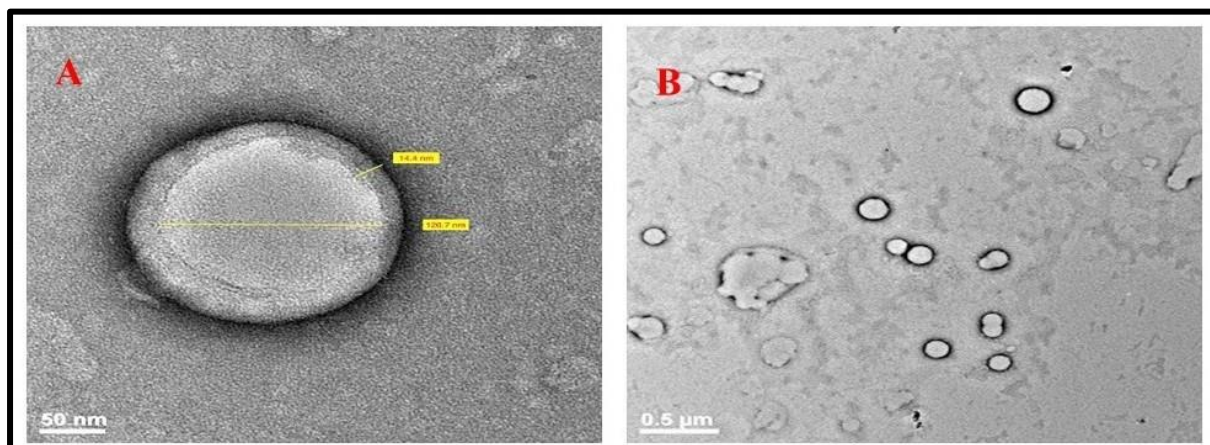


Figure 5.42 HR-TEM (a) Negative stained PLHNCs, (b) Spherical PLHNCs

5.9.4 In-vitro drug release study and drug release kinetics

Exemestane loaded PLHNCs followed the sustained release kinetics (Figure 5.45). From the three pH conditions, maximum drug release was found in pH 5.5, which suggested maximum release of the drug in cancer cells. Release of exemestane from the PLHNCs in the different media was observed to be in decreasing order of pH 5.5 > pH 6.6 > pH 7.4, which indicates least drug release in plasma and blood due to presence of DOPE, a pH dependent lipid coat which disintegrates below the pH 6.

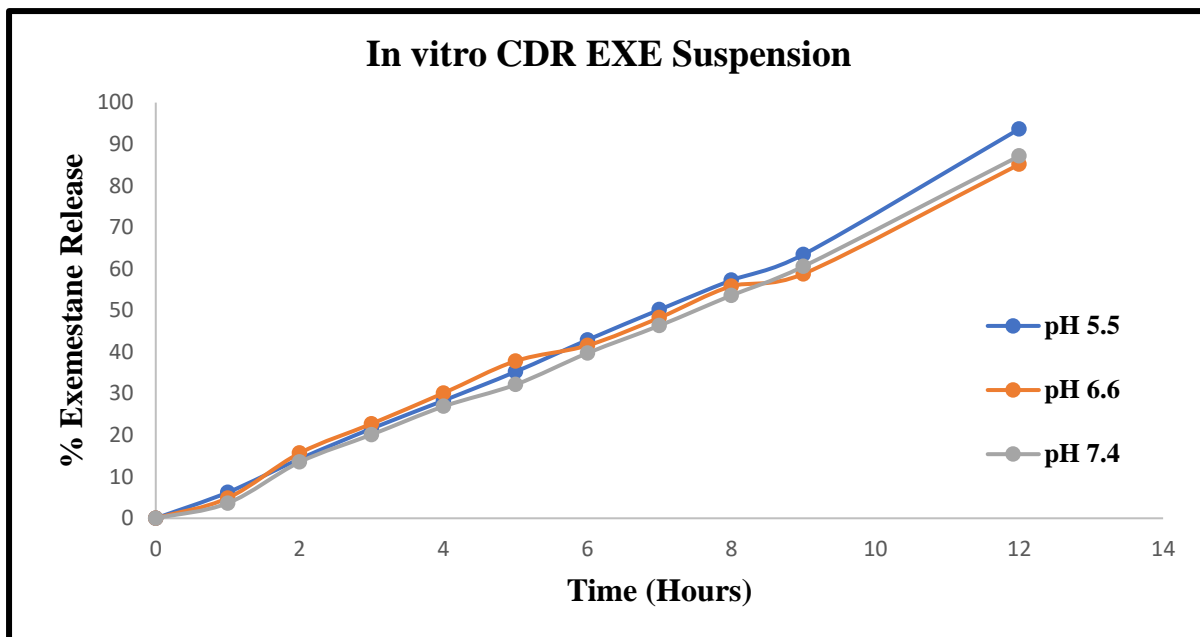


Figure 5.43 In vitro drug release of EXE suspension

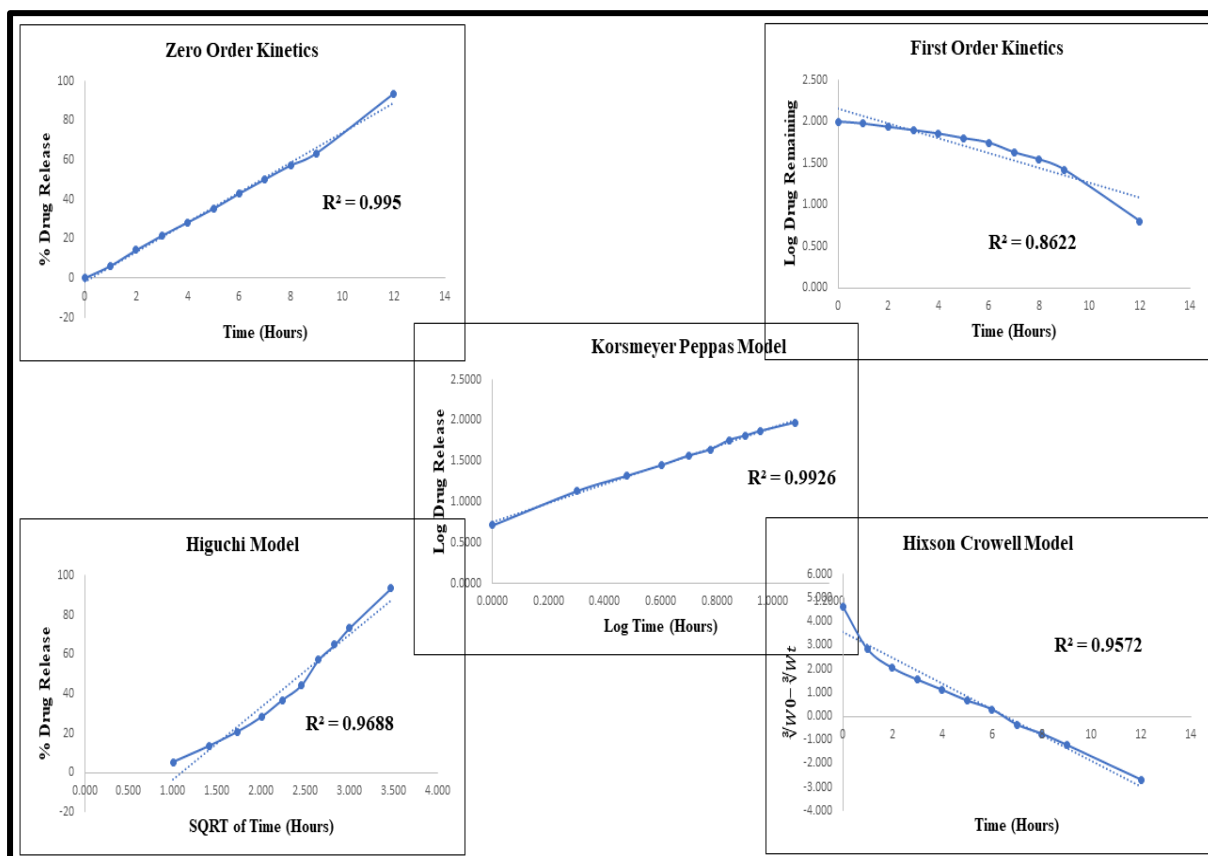


Figure 5.44 Drug release kinetics for EXE suspension

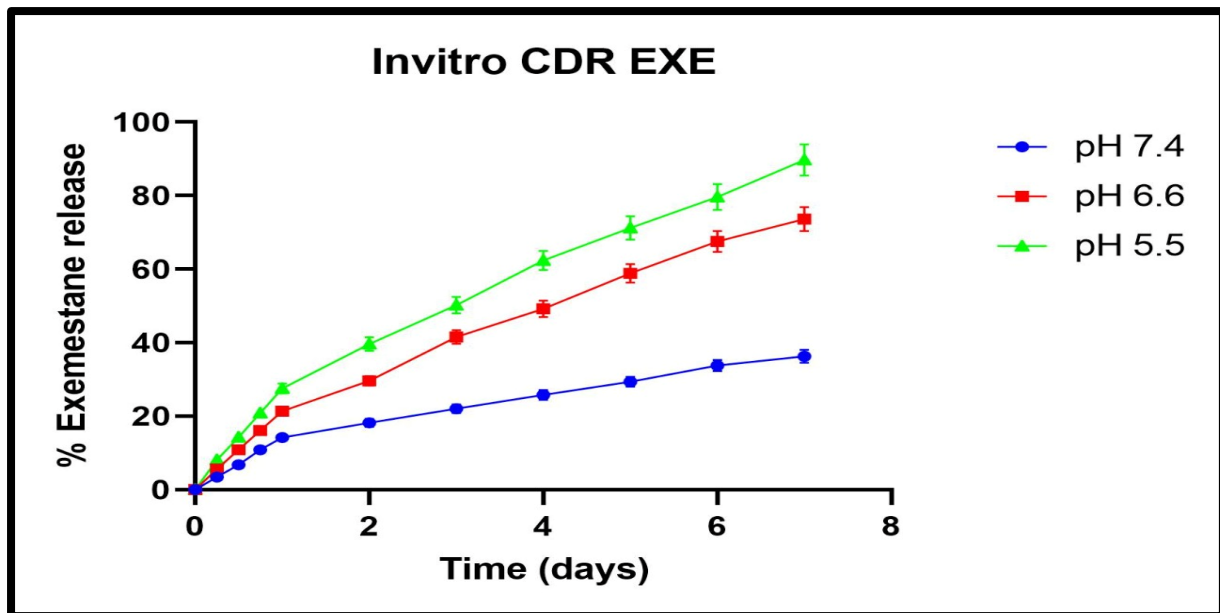


Figure 5.45 FA EXE PLHNCs drug release pattern in different release media

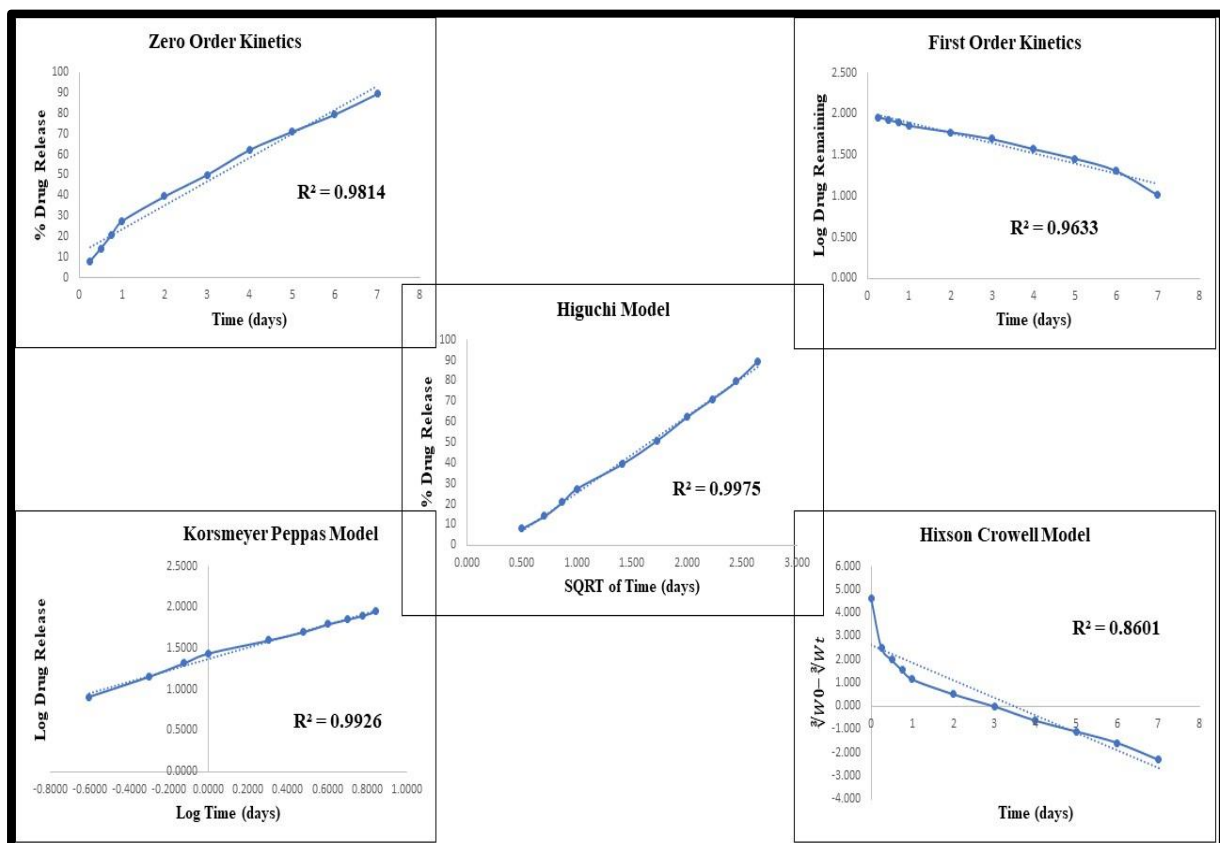


Figure 5.46 In Vitro Drug release Model kinetics for FA EXE PLHNCs

From the kinetic model fitting analysis, it was concluded that for exemestane loaded PLHNCs, the best fit model was Higuchi model (Figure 5.44) with the R^2 value of 0.9975, whereas the drug release from EXE suspension follows zero order kinetics. This shows that the drug release

from PLHNCs is matrix diffusion-controlled release process. The comparison of all the models has been given in Table 5.41.

Table 5.41 Drug release kinetics with regression coefficients

Model	FA EXE PLHNCs	EXE Suspension
Zero Order	0.9814	0.9950
First Order	0.9633	0.8622
Higuchi	0.9975	0.9688
Korsmeyer Peppas	0.9926	0.9926
Hixson Crowell	0.8601	0.9572

5.9.6 Estimation of residual solvent by Gas Chromatography

As per the ICH guidelines Q3C (R6), acetonitrile is CLASS II solvent and the permitted daily exposure limit is 4.1 mg/day which is equivalent to 410 ppm per day exposure.

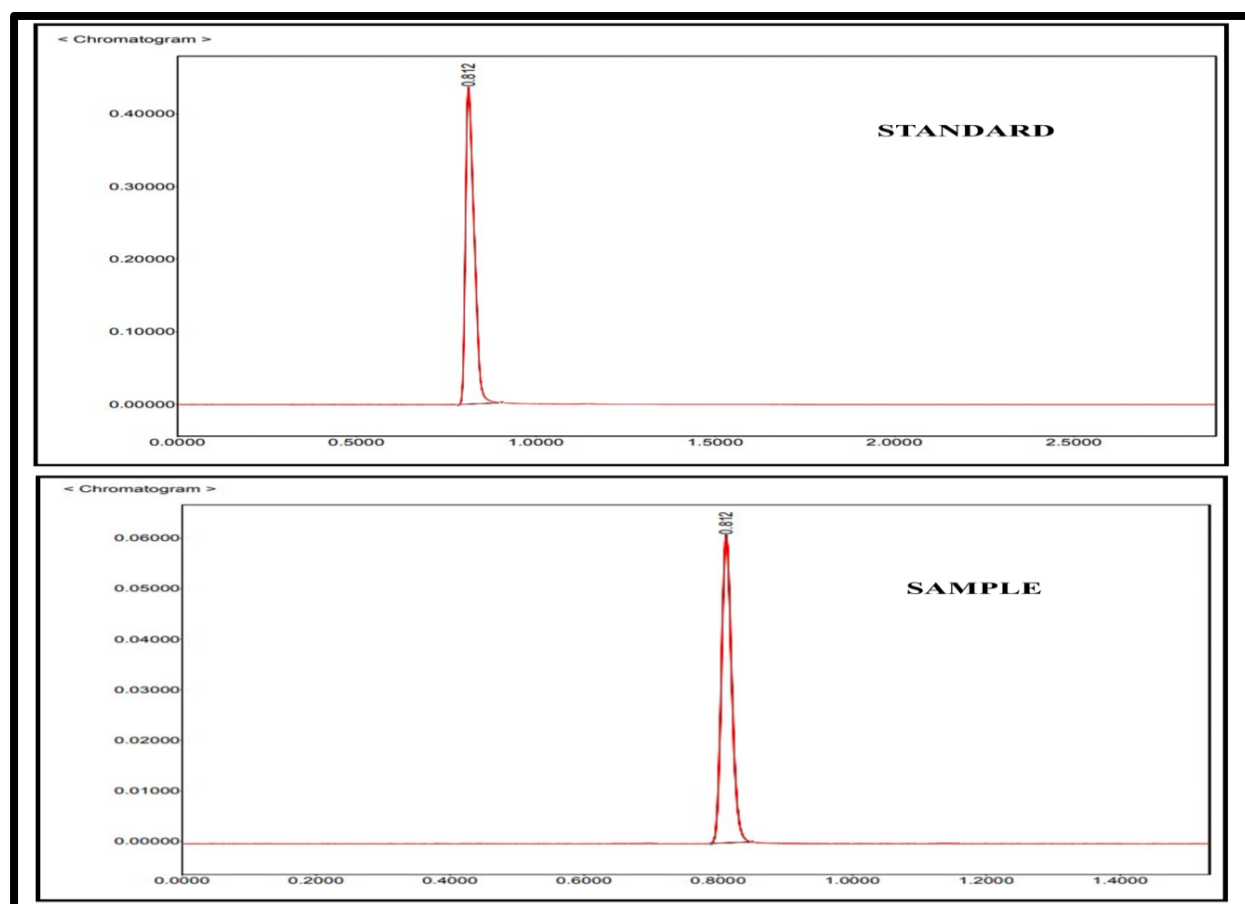


Figure 5.45 Residual Solvent Graph GC analysis

As shown in Table 5.42, it was confirmed that acetonitrile present in final optimized batch was much lower than daily limits of exposure as per ICH guidelines for residual solvents.

Table 5.42 Residual solvent analysis by GC

Sr No.	Standard Acetonitrile (ppm)	PLHNCs acetonitrile observed (ppm)	Permissible limit (ppm)
1	1000	88.72 ppm	410 ppm

References

- Sadaquat H, Akhtar M, Nazir M, Ahmad R, Alvi Z, Akhtar N. Biodegradable and biocompatible polymeric nanoparticles for enhanced solubility and safe oral delivery of docetaxel: In vivo toxicity evaluation. *International Journal of Pharmaceutics*. 2021;598:120363.
- Ma Z, Liu J, Li X, Xu Y, Liu D, He H, et al. Hydroxycamptothecin (HCPT)-loaded PEGylated lipid–polymer hybrid nanoparticles for effective delivery of HCPT: QbD-based development and evaluation. *Drug Delivery and Translational Research*. 2022;12(1):306-24.
- Savadkouhi N, Mazarei Z, Esmaeelzadeh M, Salehi P, Rafati H. Novel PEGylated Derivatives of α -Tocopherol for Nanocarrier Formulations; Synthesis, Characterization and in vitro Cytotoxicity against MCF-7 Breast Cancer Cells. *Bioorganic & Medicinal Chemistry Letters*. 2021;40:127907.
- Sivadasan D, Sultan MH, Madkhali O, Almoshari Y, Thangavel N. Polymeric Lipid Hybrid Nanoparticles (PLNs) as Emerging Drug Delivery Platform—A Comprehensive Review of Their Properties, Preparation Methods, and Therapeutic Applications. *Pharmaceutics*. 2021;13(8):1291.
- Taléns-Visconti R, Díez-Sales O, de Julián-Ortiz JV, Nácher A. Nanoliposomes in Cancer Therapy: Marketed Products and Current Clinical Trials. *International Journal of Molecular Sciences*. 2022;23(8):4249.
- Mukherjee A, Waters AK, Kalyan P, Achrol AS, Kesari S, Yenugonda VM. Lipid–polymer hybrid nanoparticles as a next-generation drug delivery platform: state of the art, emerging technologies, and perspectives. *International journal of nanomedicine*. 2019;14:1937.
- Moolakkadath T, Aqil M, Ahad A, Imam SS, Iqbal B, Sultana Y, et al. Development of transethosomes formulation for dermal fisetin delivery: Box–Behnken design, optimization, in vitro skin penetration, vesicles–skin interaction and dermatokinetic studies. *Artificial cells, nanomedicine, and biotechnology*. 2018;46(sup2):755-65.
- Mandal B, Mittal NK, Balabathula P, Thoma LA, Wood GC. Development and in vitro evaluation of core–shell type lipid–polymer hybrid nanoparticles for the delivery of erlotinib in non-small cell lung cancer. *European journal of pharmaceutical sciences*. 2016;81:162-71.

9. Godara S, Lather V, Kirthanashri SV, Awasthi R, Pandita D. Lipid-PLGA hybrid nanoparticles of paclitaxel: Preparation, characterization, in vitro and in vivo evaluation. *Materials Science and Engineering: C*. 2020;109:110576.
10. Sonam, Chaudhary H, Arora V, Kholi K, Kumar V. Effect of Physicochemical Properties of Biodegradable Polymers on Nano Drug Delivery. *Polymer Reviews*. 2013;53(4):546-67.
11. Blanco E, Shen H, Ferrari M. Principles of nanoparticle design for overcoming biological barriers to drug delivery. *Nature Biotechnology*. 2015;33(9):941-51.
12. Dong Y, Ng WK, Shen S, Kim S, Tan RBH. Preparation and characterization of spironolactone nanoparticles by antisolvent precipitation. *International Journal of Pharmaceutics*. 2009;375(1):84-8.
13. Luiz MT, Viegas JSR, Abriata JP, Viegas F, de Carvalho Vicentini FTM, Bentley MVLB, et al. Design of experiments (DoE) to develop and to optimize nanoparticles as drug delivery systems. *European Journal of Pharmaceutics and Biopharmaceutics*. 2021;165:127-48.
14. Desoqi MH, El-Sawy HS, Kafagy E, Ghorab M, Gad S. Fluticasone propionate-loaded solid lipid nanoparticles with augmented anti-inflammatory activity: Optimisation, characterisation and pharmacodynamic evaluation on rats. *Journal of Microencapsulation*. 2021;38(3):177-91.
15. Arrua EC, Sanchez SV, Trincado V, Hidalgo A, Quest AFG, Morales JO. Experimental design and optimization of a novel dual-release drug delivery system with therapeutic potential against infection with *Helicobacter pylori*. *Colloids and Surfaces B: Biointerfaces*. 2022;213:112403.
16. Köçkar H, Karaagac O. Improvement of the saturation magnetisation using Plackett–Burman design and response surface methodology: superparamagnetic iron oxide nanoparticles synthesised by co-precipitation under nitrogen atmosphere. *Journal of Materials Science: Materials in Electronics*. 2021;32(10):13673-84.
17. Fernandes RS, Raimundo Jr IM, Pimentel MF. Revising the synthesis of Stöber silica nanoparticles: A multivariate assessment study on the effects of reaction parameters on the particle size. *Colloids and Surfaces A: Physicochemical and Engineering Aspects*. 2019;577:1-7.
18. Peña-Parás L, Rodríguez-Villalobos M, Maldonado-Cortés D, Guajardo M, Rico-Medina CS, Elizondo G, et al. Study of hybrid nanofluids of TiO₂ and montmorillonite clay nanoparticles for milling of AISI 4340 steel. *Wear*. 2021;477:203805.
19. Bhattacharya S. Methotrexate-loaded polymeric lipid hybrid nanoparticles (PLHNPs): a reliable drug delivery system for the treatment of glioblastoma. *Journal of Experimental Nanoscience*. 2021;16(1):344-67.
20. Sengel-Turk CT, Ozkan E, Bakar-Ates F. Box-Behnken design optimization and in vitro cell based evaluation of piroxicam loaded core-shell type hybrid nanocarriers for prostate cancer. *Journal of Pharmaceutical and Biomedical Analysis*. 2022;216:114799.
21. Mahmood S, Kiong KC, Tham CS, Chien TC, Hilles AR, Venugopal JR. PEGylated lipid polymeric nanoparticle-encapsulated acyclovir for in vitro controlled release and ex vivo gut sac permeation. *Aaps Pharmscitech*. 2020;21(7):1-15.

22. Shihab SK. Optimization of WEDM process parameters for machining of friction-stir-welded 5754 aluminum alloy using Box–Behnken design of RSM. *Arabian Journal for Science and Engineering*. 2018;43(9):5017-27.
23. Barabadi H, Honary S, Ebrahimi P, Alizadeh A, Naghibi F, Saravanan M. Optimization of myco-synthesized silver nanoparticles by response surface methodology employing Box–Behnken design. *Inorganic and Nano-Metal Chemistry*. 2019;49(2):33-43.
24. Bahari NA, Isahak WNRW, Masdar MS, Ba-Abbad MM. Optimization of the controllable crystal size of iron/zeolite nanocomposites using a Box–Behnken design and their catalytic activity. *Applied Nanoscience*. 2019;9(2):209-24.
25. Dash AR, Lakhani AJ, Devi Priya D, Surendra TV, Khan MMR, Samuel E, et al. Green Synthesis of Stannic Oxide Nanoparticles for Ciprofloxacin Degradation: Optimization and Modelling Using a Response Surface Methodology (RSM) Based on the Box–Behnken Design. *Journal of Cluster Science*. 2021:1-13.
26. Habib BA, Abdeltawab NF, Salah Ad-Din I. D-optimal mixture design for optimization of topical dapson e niosomes: in vitro characterization and in vivo activity against *Cutibacterium acnes*. *Drug Delivery*. 2022;29(1):821-36.
27. Mandal SK, Ojha N, Das N. Optimization of process parameters for the yeast mediated degradation of benzo [a] pyrene in presence of ZnO nanoparticles and produced biosurfactant using 3-level Box-Behnken design. *Ecological Engineering*. 2018;120:497-503.
28. Fernandes RS, Silva JO, Seabra HA, Oliveira MS, Carregal VM, Vilela JMC, et al. α -Tocopherol succinate loaded nano-structured lipid carriers improves antitumor activity of doxorubicin in breast cancer models in vivo. *Biomedicine & Pharmacotherapy*. 2018;103:1348-54.
29. Fröhlich E. The role of surface charge in cellular uptake and cytotoxicity of medical nanoparticles. *International journal of nanomedicine*. 2012;7:5577.
30. Kushwah V, Katiyar SS, Agrawal AK, Gupta RC, Jain S. Co-delivery of docetaxel and gemcitabine using PEGylated self-assembled stealth nanoparticles for improved breast cancer therapy. *Nanomedicine: Nanotechnology, Biology and Medicine*. 2018;14(5):1629-41.